



DEGREE PROJECT IN MASTER'S PROGRAMME, ENGINEERING DESIGN
120 CREDITS, SECOND CYCLE
STOCKHOLM, SWEDEN 2015

Design and implementation of a fault tolerant vehicle controller - an active steering approach

STEFANOS KOKOGIAS

KTH ROYAL INSTITUTE OF TECHNOLOGY

SCHOOL OF INDUSTRIAL ENGINEERING AND MANAGEMENT

TRITA Stefanos Kokogias MMK 2015:67 MDA 508

 KTH VETENSKAP OCH KONST	Examensarbete MMK 2015:67 MDA 508 Design and implementation of a fault tolerant controller on a prototype vehicle, using an active steering approach.	
Stefanos Kokogias		
Godkänt 2015-06-17	Examinator Martin Törngren	Handledare Sagar Behere, Micke Hellgren
	Uppdragsgivare Mikael Nybacka	Kontaktperson Stefanos Kokogias

Sammanfattning

KTH har utvecklat ett nytt konceptfordon för forskning baserat på ”autonoma hörnmoduler”. En autonom hörnmodul består av ett hjul med en inbyggd elektrisk motor och aktuatorer för att kontrollera lutning och styrvinkel. En modul är monterad i varje hörn av ett ”skateboard-chassi”. Tillsammans med ett batteri och en dator som styr dessa hörnmoduler fås ett fordon med en helt elektrisk drivlina. Den här konstruktionen ger stora fördelar med avseende på fordonets dynamiska egenskaper men det uppkommer också svåra säkerhetsfrågor på grund av att hörnmodulerna kan styras individuellt.

Det här examensarbetet fokuserar på designen av en feltolerant regulator och dess implementation i fordonet. De fel som har studerats är fel såsom att motorn i en hörnmodul eller aktuatorerna för lutning och styrvinkel slutar att fungera, dessa fel kan skapa en oönskad rotation av fordonet. Den föreslagna kontrollern består av två delar, en del kontrollerar det drivande momentet hos de olika modulerna och den andra består av aktiv styrning av fordonets rotationshastighet utifrån en given referens. Den föreslagna kontrollern utnyttjar fördelarna från båda delsystemen för att ge ingenjörerna en större möjlighet att uppnå en bättre styrbarhet av fordonet.

Den föreslagna regulatorn uppvisade lovande resultat i simuleringar men på grund av ett mekaniskt fel i en av hörnmodulernas motorer utfördes experiment enbart med den aktiva styrningen. Denna kunde framgångsrikt upphäva felets negativa effekt på fordonets styrförmåga.

 KTH VETENSKAP OCH KONST	Master of Science Thesis MMK 2015:67 MDA 508 Design and implementation of a fault tolerant controller on a prototype vehicle, using an active steering approach.	
Stefanos Kokogias		
Approved 2015-06-17	Examiner Martin Törngren	Supervisor Sagar Behere, Micke Hellgren
	Commissioner Mikael Nybacka	Contact person Stefanos Kokogias

Abstract

KTH has developed a novel Research Concept Vehicle (RCV) based on the concept of "*autonomous corner modules*". An autonomous corner module is basically a wheel with a built-in electric hub motor, and additional actuators to tilt and yaw the wheel. One module is attached at each of the four corners of a 'skateboard' chassis. The addition of a computer to command each corner module, and a battery, results in a vehicle with a completely electric drive train. This topology can provide major advantages with respect to the dynamic behavior of the RCV. On the contrary, major safety issues arise from the individual controllability of the corner modules.

This thesis is mainly focused on the design of a fault tolerant controller and its implementation on the RCV. The faults that are being considered include on board system failures i.e. hub-motor or steering actuator failure, all of which can induce unintended yaw rate in the vehicle's response. The proposed controller includes the use of a torque allocation approach combined with an active steering approach which constantly compensate for any divergence in the vehicle's yaw rate response from the reference. This controller utilizes the advantages of both yaw rate control mechanisms enabling the engineers to achieve better vehicle response. Finally, the aforementioned controller showed encouraging results in simulation but due to a mechanical failure in one of the four hub-motors, experimental tests were only conducted using the active steering controller which successfully suppressed the failure's negative effect on the vehicle's response.

Acknowledgements

At this point I would like to express my deep gratitude to Propondis Foundation for awarding me with a 2 year scholarship, without which it would not be possible for me to study in KTH for the past two years. Also, I would like to thank Sagar Behere and Micke Hellgren for their support and mentoring throughout this project, Mikael Nybacka and Daniel Wanner for all the valuable information concerning the project and finally, Peter Tomner for his technical support.

Contents

Sammanfattning	i
Abstract	iii
Acknowledgements	v
Contents	vii
List of Figures	x
List of Tables	xiii
Abbreviations	xiv
Symbols	xv
1 Introduction	1
1.1 Background	1
1.1.1 Introduction	1
1.1.2 Fault detection and classification	2
1.2 System description	3
1.3 Delimitations	4
1.3.1 Limitations on ISO 26262 use	4
1.3.2 Fault detection	4
1.3.3 Availability issues	5
1.4 Thesis scope	6
1.5 Methods	6
1.6 Research questions	7
1.7 Ethical aspects	8
2 Frame of reference	9
2.1 Fault-tolerant control	10
2.2 Fault handling through Tyre-Force allocation	11
3 Initial problem analysis	16
3.1 Fault consequences	16
3.1.1 Drive shutdown	17

3.1.2 Inverted torque	17
3.1.3 Wheel lock	20
3.2 Additional faults related to fail-operational analysis	20
3.3 Fault selection	22
3.4 Yaw rate control mechanisms	23
3.5 Active steering	24
3.6 Fault handling approaches and change of scope	24
3.7 ISO 26262 delimitations	25
4 Implementation	28
4.1 Practical implementation	28
4.1.1 IMU installation	28
4.1.2 Fault induction setup	30
4.2 ASIL assignment	31
4.3 Modeling	33
4.3.1 Steering actuators	33
4.3.2 Bicycle model	35
4.3.3 Vehicle model	38
4.3.4 Model	42
4.4 Control	43
4.4.1 Controller design criteria	43
4.4.2 Steering controller	44
4.5 Testing	46
4.5.1 Safety measures	46
4.5.2 Testing limitations	47
5 Results	48
5.1 Simulated results	48
5.2 Measured results	50
5.2.1 Braking torque induction	50
5.2.2 Wheel lock	52
5.2.3 Disabling one steering actuator	53
6 Discussion and conclusions	56
6.1 Discussion	56
6.2 Conclusions	57
7 Recommendations and Future work	62
7.1 Recommendations	62
7.2 Future work	63
A Appendix - Simulated results	66
B Appendix B - Experimental results	74

C Appendix C - Fault list	82
D Appendix D - Simulink model used in RCV	85
Bibliography	90

List of Figures

1.1	RCV chassis	2
1.2	RCV chassis	3
1.3	RCV and dSPACE availability timeplan	5
2.1	RCV dynamics	12
3.1	Measured yaw response of the RCV during motor-drive shutdown	17
3.2	Measured yaw rate response of the RCV during the induction of 50Nm breaking torque on rear left wheel	18
3.3	Measured yaw rate response of the RCV during the induction of 100Nm breaking torque on rear left wheel	19
3.4	Measured motor torques (to the left) and wheel velocities (to the right) during the induction of a 50Nm breaking torque on rear left wheel	19
3.5	Measured motor torques (to the left) and wheel velocities (to the right) during the induction of a 100Nm breaking torque on rear left wheel	19
3.6	Measured yaw response of the RCV during wheel lock	20
3.7	Thesis fault handling approach	25
3.8	V model overview of ISO 26262	26
4.1	Functional flow chart of the dynamic DC offset compensation algorithm	29
4.2	Compensation of DC offset using the sequential compensation algorithm	30
4.3	GPS antennas and IMU placement	31
4.4	Fitting of the steering actuator model	35
4.5	Validation of the steering actuator model	36
4.6	Bicycle model	36
4.7	Bicycle look-up table Simulink diagram	37
4.8	A bicycle model validation test with constant steering and increasing velocity is conducted (to the left) and a test with induced faults during driving (to the right)	38
4.9	A bicycle model validation test with constant steering and increasing velocity is conducted (to the left) and a test with slalom driving maneuvers (to the right)	38
4.10	Constant steering increasing velocity test	40

4.11	Model validation on a test case with motor shut down fault induced on the vehicle.	40
4.12	Model validation on test case with braking torque fault induced on the vehicle.	41
4.13	Model validation on test case with braking torque fault induced on the vehicle, showing faulty condition behavior.	41
4.14	Complete Simulink model diagram	42
4.15	Steering controller block diagram	45
5.1	Yaw rate response of the vehicle for the different control strategies.	49
5.2	Induction of a 100 Nm breaking torque on the rear left wheel	51
5.3	Locking the rear left wheel	52
5.4	Deactivating the front right steering actuator	53
5.5	Deactivating the front right steering actuator	54
5.6	Measured and reference yaw rate zoomed	54
6.1	Ackerman angles calculation	60
A.1	Response of the vehicle when braking torque is induced on the rear left wheel	66
A.2	Response of the vehicle when braking torque is induced on the rear left wheel while the steering controller is active.	67
A.3	Response of the vehicle when braking torque is induced on the rear left wheel while both steering and torque allocation controllers are active.	68
A.4	Response of the vehicle when braking torque is induced on the rear left wheel while both controllers are active and torque allocation's control signal is integrated in the steering controller.	69
A.5	Response of the vehicle when the rear left wheel is locked.	70
A.6	Response of the vehicle when the rear left wheel is locked while the steering controller is active.	71
A.7	Response of the vehicle when the rear left wheel is locked while both steering and torque allocation controllers are active.	72
A.8	Response of the vehicle when the rear left wheel is locked while both controllers are active and torque allocation's control signal is integrated in the steering controller.	73
B.1	Negative torque inductions test, yaw rate error	75
B.2	Negative torque inductions test, steering signals	75
B.3	Negative torque inductions test, motor torque	76
B.4	Inverted torque fault induction response without a controller	76
B.5	Inverted torque fault induction response without a controller	77
B.6	Inverted torque fault induction response without a controller	77
B.7	Inverted torque fault induction response without a controller	78
B.8	Inverted torque fault induction response without a controller	78
B.9	Inverted torque fault induction response without a controller	79
B.10	Inverted torque fault induction response without a controller	79
B.11	Inverted torque fault saadinduction response without a controller	80

B.12 Inverted torque fault fdainduction response without a controller	80
B.13 Inverted torque fault iagnduction response without a controller	81
B.14 Measured and reference yaw rate zoomed	81
D.1 Steering controller block	86
D.2 Pseudo-inverse block.	87
D.3 Torque allocation blocks.	88
D.4 IMU data receive block.	89

List of Tables

3.1	A table consisting the faults that are going to be further analyzed concerning fault handling	22
3.2	ISO 26262 coding and modeling guidelines	27
4.1	Areas of lateral acceleration for normal driving	32
4.2	ASIL level derivation table	34
C.1	List of fault groups 1-3.	83
C.2	List of fault groups 4-7.	84

Abbreviations

ASIL	Automotive Safety Integrity Level
AFTC	Active Fault Tolerant Control
CAN	Controller Area Network
CoG	Center of Gravity
ECU	Electronic Control Unit
E/E	Electrical/Electronic
EM	Electric Motors
GPS	Global Positioning System
IMU	Inertia Measurement Unit
ISO	International Organization of Standardization
ITRL	Integrated Transport Research Lab
PFTC	Passive Fault Tolerant Control
PID	Proportional Integral Derivative
RCV	Research Concept Vehicle
SA	Steering Actuators
SC	Steering Control
TA	Torque Allocation
WAS	Wheel Active Steering
WCS	Worst Case Scenario

Symbols

δ	Tire angle	<i>rad</i>
$\dot{\psi}$	Yaw rate	<i>rad/s</i>
l_f	Distance between the front wheels' axle and the CoG	m
l_r	Distance between the rear wheels' axle and the CoG	m
s_r	Track width	m
F_x	Longitudinal Force	N
F_y	Lateral Force	N
M_z	Torque around the Z-axis	Nm
u_x	Longitudinal velocity	<i>m/s</i>
u_y	Lateral velocity	<i>m/s</i>

Chapter 1

Introduction

In this chapter the background, purpose, limitations and method will be described. Additionally, a short description of the vehicle's setup is presented and the research questions and thesis' contributions are stated.

1.1 Background

1.1.1 Introduction

KTH has developed a novel Research Concept Vehicle (RCV) based on the concept of "*autonomous corner modules*". An autonomous corner module is basically a wheel with a built-in electric hub motor and additional actuators to tilt and yaw the wheel. One module is attached at each of the four corners of a 'skateboard' chassis. The addition of a computer to command each corner module and a battery, results in a vehicle with a completely electric drive train.

This topology can provide major advantages in terms of energy efficiency, safety and performance, enabling the engineers to improve the vehicle's behavior. On the contrary, major safety issues arise from the individual controllability of the corner modules.

One of KTH:s ambitions is to make the RCV autonomous i.e. self-driving. To achieve that goal, one of the tasks is to create (computer based) systems that can

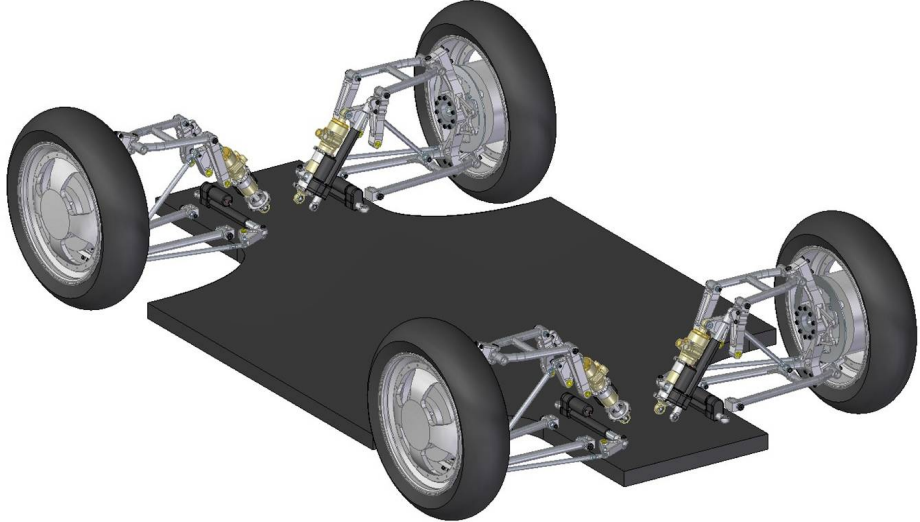


FIGURE 1.1: RCV wheels and chassis CAD

detect faults happening in the vehicle, as it is being driven, and then handle the situation in a safe way.

At the moment, a set of faults that need to be detected and handled have been identified. However, the actual mechanisms of detecting all those faults in a running vehicle have not yet been created. Also, there is a lack of knowledge regarding how each of the identified faults should be dealt with, during each operating condition that the fault can occur in. The impact of the faults on the control strategies that already exist for the vehicle (which assume a fault free vehicle) therefore needs to be studied.

1.1.2 Fault detection and classification

As already mentioned, a set of faults that need to be detected and handled have been identified. These faults were derived in [4], where a failure mode analysis has been carried out for the driveline of electric and hybrid vehicles in order to make a classification of the faults that can occur. The list of faults that was used for this thesis, was chosen from an alternate version of the aforementioned publication and is focused on faults that could occur on the electric motors of the RCV. The choice of specific faults was done at the beginning of this project and was based on two criteria namely, the fault's severity and relativity to the student's background. In tables C.1 and C.2, the list of faults that are going to be

investigated on this thesis concerning detection and handling is presented. In this list, a number of parameters related to the faults are presented, including "Failure effect" and "Potential causes".

1.2 System description

As stated in chapter 1, the RCV is a laboratory vehicle which incorporates many advanced topologies like, torque control on each wheel independently using one in-wheel motor on each wheel, steer-by-wire system and camber adjustment, for the improvement of the dynamic behavior of the vehicle.

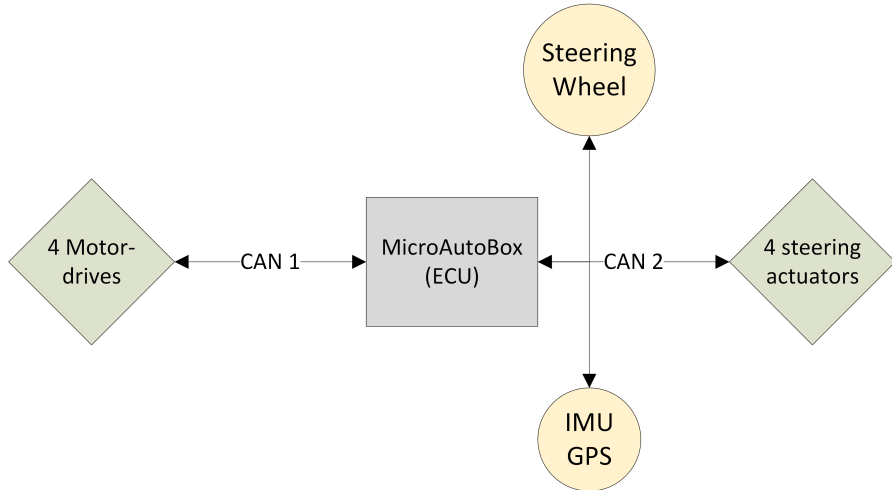


FIGURE 1.2: RCV communication diagram

More specifically, four Kollmorgen ACD 4805 motor drives are used to power the hub motors of the RCV which exchange data with the main ECU through CAN. Also, the steering is achieved by utilizing four linear actuators EPOS 70/10. The steering actuators use a second CAN network where the GPS-IMU sensor is also connected for communication with the main ECU. Finally, the main ECU is a MicroAutoBox that is manufactured by dSPACE. This architecture can also be seen in figure 1.2. More specific information about the vehicle, its apparatus and its functionality can be found in [13].

1.3 Delimitations

1.3.1 Limitations on ISO 26262 use

As can be seen in [3.8](#) and through the study of ISO 26262 standard, the analysis of automotive safety is a process that starts from the concept phase and extends to the decommissioning of the vehicle. Thus, it is mainly designed to be adopted by the industry for the design of conventional vehicles, which does not apply for the RCV's case. Since safety analysis using ISO 26262 was in this thesis' initial description, a lot of effort was spent to find possible ways to incorporate ISO's methodology to the RCV. Unfortunately, since the RCV is an already built prototype vehicle and is composed of "black box" components on which our intervention (on software or hardware level) is difficult and impractical, the use of ISO 26262 was deemed inapplicable. As a result, it was limited to suggestions for future implementation and the assignment of the ASIL levels to the different hazards that can arise due to a fault. More information on this subject can be found in chapter [3.7](#).

1.3.2 Fault detection

For the detection of the faults that were going to be studied and given that the motor drives have a built-in fault detection mechanism, the system's fault detection abilities were studied. It was concluded that many of the chosen faults could be detected by the drives. Unfortunately, some of the most severe faults are not detectable by the current drive fault detection mechanism. These faults can be seen in fault groups 5 and 6 in table [C.2](#) and they include mechanical failures and sensor's malfunction. As a consequence, it was suggested that additional hardware would be installed in order to detect these faults, but since the motor-drive system is a black box and its functionality is unknown, any intervention was deemed impractical and irrelevant to this thesis' scope. Hence, the only hardware changes that were implemented during this thesis were those that were already scheduled for the RCV by the ITRL administration and were mainly focused on the vehicle's functionality.

1.3.3 Availability issues

Another major limitation that affected the scope and results of this thesis, was the vehicle's availability issues which can be seen in figure 1.3. It should be noted here that the dates are not accurate but rather represent a time period of a few days for each milestone.

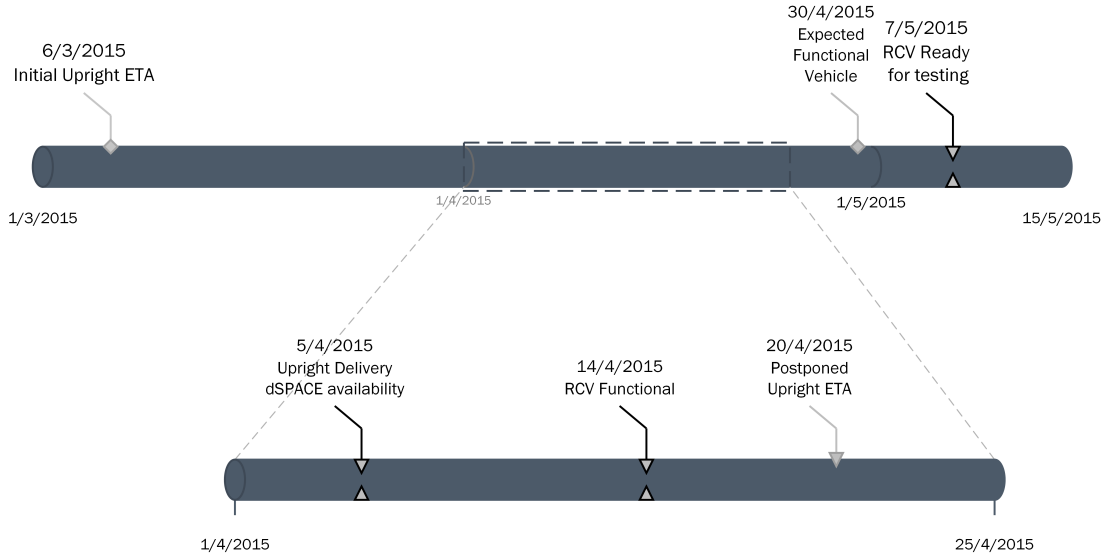


FIGURE 1.3: RCV and dSPACE availability timeplan

Upon the start of this thesis, the RCV was unavailable since it was missing its uprights. At that point, it was planned that the new upright order would be delivered on the beginning of March. Unfortunately, due to delays on the parts design, the date was pushed back to the mid of April. Since experience has shown that usually these deadlines are not met and given that these parts were ordered more than a year ago and hadn't been delivered yet, the thesis' time plan was set to expect the uprights at the end of April. Thus, the full functionality of the RCV was expected in the beginning or middle of May. That led to the decision that, since the vehicle is not going to be functional until that time, there was a big possibility that there will not be enough time to conduct any tests on the real vehicle. Hence, the whole thesis was redirected to a more modeling and simulation approach which (in order to be useful for future use) would require to be accurate and realistic. As a result, the tuning of the existing models to the parameters of the real vehicle, was necessary.

Surprisingly enough, the uprights were delivered in the beginning of April which was a major change at the time and shifted the thesis' scope to the implementation of the controller on the RCV. Finally, a very important tool that arrived the same period as the uprights was the computer that had the dSPACE license and was used on a different project. More information on this subject can be found in chapter 4.3.

All these aforementioned limitations led to a gradual change of scope which will be further analyzed in 3.6.

1.4 Thesis scope

An important part of work in this thesis was focused on the scope determination. Although the reasons and the process which led to the scope change is further analyzed in chapter 3.6, the finalized version is presented here for clarity reasons. This finalized version focuses on the development and implementation of a fault tolerant controller for the RCV which will compensate for the initially chosen faults. More specifically, through the development of corresponding controllers for the steering actuators and the hub-motors, a fault tolerant controller will be introduced which will compensate for the faulty conditions without the use of fault detection mechanisms.

1.5 Methods

The three main methods used were modeling, simulation and experimental validation. As mentioned in chapter 1.3, modeling and simulation methods were used to compensate for safety and vehicle's availability issues.

Since the vehicle was not expected to be available until the middle of May, there was a need for a realistic model that would result in reliable results. In order to achieve that, and since the proposed fault compensation scheme included an active steering controller, the derivation of a model was necessary. That led to the derivation of a steering actuator model and the tuning of a bicycle model and

complex vehicle model which already existed. Also, most obvious reasons in control engineering, namely safety and efficiency, were addressed through simulation. Having a realistic model that described the vehicle's behavior in an acceptable way, reduced the effort and risk exposure immensely. After finalizing the fault compensation controller in simulation, it was necessary to verify these results on the real vehicle through experimental validation.

1.6 Research questions

In this section, the research questions initially stated in the thesis description, as well as research questions which emerged in the course of work are stated. Most of the answers are given in different parts of this report, and will be compiled in chapter 6.2. At this point, it is important to be noted that from the initial list of faults chosen for this project, only the most severe were chosen for further analysis, leading to a refined list of three main fault groups which are presented in sub chapter 3.3.

Question 1: How can the chosen faults be detected? Identify the obstacles to overcome in order to achieve fault detection and what support is needed from the vehicle E/E architecture to aid fault detection.

Question 2: How can the chosen faults be handled so as to minimize risk to driver, vehicle and surroundings? Identify the obstacles to overcome in order to achieve this and what support is needed from the electrical/electronic (E/E) architecture for executing the fault handling.

Question 3: Is the vehicle fail operational when the vehicle experiences unintended yaw rate?

Question 4: Is the active steering approach which was implemented in this thesis (and is described in chapter 4.4.2), a viable solution for fault compensation in conventional vehicles?

1.7 Ethical aspects

It is well known that the modern world suffers great losses from car accidents. The consequences of such events can have social impact (mental impact to families, relatives etc), financial impact (health care expenses etc) and environmental impact(energy wasted in the disposal of a destroyed vehicle and the manufacture of a new one).

Since safety is the main topic of interest in this thesis, a possible implementation of such fault tolerant mechanisms in conventional vehicles can lead to a reduction of accidents caused by vehicle faults. Unfortunately, the proposed fault handling approaches cover a wide range of yaw control mechanisms which conventional vehicles cannot use. Also, the steer-by-wire technology is not very popular yet, but it will hopefully be adopted by the automotive industry in the future. Hence, the prospect of a socially sustainable solution is postponed further into the future, given that even if steer-by-wire is adopted by the automotive industry, only luxury cars will be equipped with it (initially at least). Finally, for the reasons presented previously, this technology is both financially and environmentally sustainable.

A different ethical aspect that is of concern in this thesis, is safety measures during testing. More information about safety measures, is presented in chapter [4.5.1](#).

Chapter 2

Frame of reference

This chapter presents the theoretical frame reference that is necessary for the performed research. More specifically, the work that had already been conducted prior to this thesis and constitute the basis for further implementation will be presented. The two main areas of interest are:

- Fault-tolerant control [3]
- Fault handling [1]

Additionally, a lot of research has been conducted through the past years on this vehicle. A series of publications has been conducted by Daniel Wanner which are well connected to this thesis and set the basis for further implementation. These publications concern tire-force allocation techniques [1], fault-tolerant systems analysis [2], fault classification and fault compensation [3], [4]. Also, valuable information was derived from [5] where the possible faults that can arise in a permanent magnet synchronous motor are analyzed and from [6] where there is an extensive analysis detailing information about the design of the RCV.

Also, since an active steering approach was chosen to be implemented for this thesis, an extended search for publications on this matter was conducted. More specifically, 2 wheel active steering (WAS) and 4WAS systems are presented here [7], where a sliding mode controller is presented for front 2WAS, rear 2WAS and 4WAS; and here [8], where another 4WAS approach using sliding mode control

is presented. Interestingly enough, the sliding mode approaches are very popular amongst steering controllers (S.C.) since they provide model robustness and non-linearity compliance. The aforementioned reasons led to the serious examination of a sliding mode controller for the active steering.

In the field of control allocation, the most common allocation techniques like pseudo-inverse, quadratic programming and fixed-point methods are presented in [9] and [10]. Moreover, an extended survey about the different control allocation algorithms can be found in [11].

Finally, one of the goals was the derivation of the Automotive Safety Integrity Levels (ASIL) which represent an automotive-specific risk-based classification of a safety goal as well as the validation and confirmation measures required by the ISO 26262 standard to ensure accomplishment of that goal. In order to achieve this, a publication of the U.S. Department of Transportation [12] was used in order to have a better understanding of the severity factors and the fidelity rates of automotive accidents in urban areas. All this work and other unpublished reports about the RCV are the basis for the implementation of this thesis and were extensively studied.

2.1 Fault-tolerant control

As is elaborated in [2], the goal of fault-tolerant systems is to remain operational even when one or more faults are present. More specifically, fault-tolerant systems need to (depending on the severity of the fault) continue being fully functional or having an acceptable degradation in functionality after the occurrence of failure of one or more of its components. In order to achieve this, fault-tolerant systems need *redundancy* and *quality oriented holistic design process*.

Redundancy is utilized to provide to the system the ability to continue its function until it comes to a safe state. Redundancy can be reached through the addition of either software or hardware components which would have the same or similar functionality to the systems that they are going to replace in case of failure. During the design process, different methods are used in order to achieve fault-tolerance.

Such methods are reliability analysis, hazard analysis event and fault tree analysis or failure mode effect analysis.

Fault-tolerant control techniques are mainly divided into two categories; active and passive. *Passive fault-tolerant control* (PFTC) strategies react on a specific group of fault modes. Its behavior is fixed and predefined during the controller's design which can affect negatively its fault-tolerant characteristics when it comes to an unexpected fault which was not considered during the design process. On the contrary, *active fault-tolerant control* (AFTC) strategies react to the occurrence of faults by either selecting one of predefined controllers or by synthesizing one on-line.

2.2 Fault handling through Tyre-Force allocation

As discussed in chapter 1 and is further elaborated in [1], topologies like the in-wheel motors and steer-by-wire can be very beneficial when it comes to adjusting the dynamic behavior of the vehicle. Hence, this ability of the RCV can be utilized to achieve a fault-tolerant behavior. In this chapter, a tyre-force allocation scheme is presented. This approach, utilizes the ability of the RCV to allocate torque independently on its four in-wheel motors. By appropriately allocating the torque on its four motors, the vehicle can achieve yaw rate compensation. In figure 2.1, the dynamic model of a 4 wheel-drive (4WD), front wheel steering (FWS) vehicle is presented.

In figure 2.1, f'_{xi} is the longitudinal tire force, f_{xi} is the longitudinal chassis force, f'_{yi} is the lateral tire force, f_{yi} is the lateral chassis force, α_i is the tire slip angle and δ_i is the steering angle. The DOF that need to be modeled and controlled on the RCV are three, namely longitudinal motion, lateral motion and yaw motion. The forces that are applied on the CoG and correspond the aforementioned DOF, are the longitudinal force (F_x), the lateral force (F_y) and the torque applied on the vertical axis (M_z), respectively. The utilized actuators to manipulate these motions, are four. Systems such as this, where the number of actuators is bigger than the number of controlled variables, are called over-actuated.

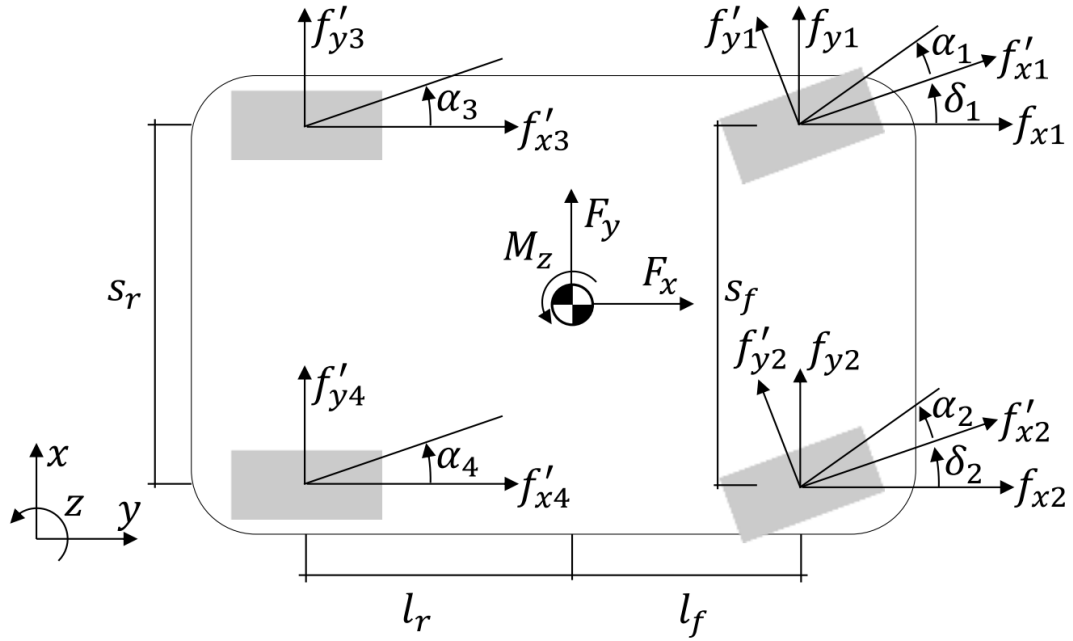


FIGURE 2.1: Vehicle's dynamic model

There are two main approaches which have been analyzed in order to be implemented on the RCV, the *Moore-Penrose pseudo-inverse control allocation* and the *Optimal Control approach*.

The *Pseudo-Inverse approach*, is the calculation of the minimal solution in terms of the least square error. The main characteristics of this approach are the following:

- Low computation power needed
- Easy and straightforward implementation
- Constraints are not respected-considered

The last characteristic is the one major disadvantage of this technique since without proper care, the allocator will saturate the actuators when there is need for high yaw rate compensation.

The relation here between $F_{veh}^{ref} = [F_x^{ref} M_z^{ref} 0]^T$ and forces on the longitudinal $f_x'^{ref} = [f_{x1}'^{ref} f_{x2}'^{ref} f_{x3}'^{ref} f_{x4}'^{ref}]^T$ and lateral $f_y'^{ref} = [f_{y1}'^{ref} f_{y2}'^{ref} f_{y3}'^{ref} f_{y4}'^{ref}]^T$ direction is given by:

$$F_{veh}^{ref} = A' f_y'^{ref} + B' f_x'^{ref} \quad (2.1)$$

where the longitudinal tyre matrix is

$$B' = \begin{bmatrix} \cos(\delta_1) & \cos(\delta_2) & 1 & 1 \\ -\frac{s_f \cos(\delta_1)}{2} + l_f \sin(\delta_1) & \frac{s_r \cos(\delta_2)}{2} + l_f \sin(\delta_2) & -\frac{s_r}{2} & \frac{s_r}{2} \\ k_{f,1} & k_{f,2} & k_{f,3} & k_{f,4} \end{bmatrix} \quad (2.2)$$

and lateral tyre matrix is

$$A' = \begin{bmatrix} -\sin(\delta_1) & -\sin(\delta_2) & 0 & 0 \\ \frac{s_f \sin(\delta_1)}{2} + l_f \cos(\delta_1) & -\frac{s_r \sin(\delta_2)}{2} + l_f \cos(\delta_2) & -l_r & -l_r \end{bmatrix} \quad (2.3)$$

Here, δ_i is the steering angle and l_f and l_r are the distances of the CoG from the front and rear wheel axles respectively. In the approach currently used in RCV, the lateral tyre forces are assumed non-controllable and are thus disregarded. The longitudinal tyre forces though are found by calculating the pseudo-inverse of matrix B' . Finally, on the third row of matrix B' , there is a fault-activated variable $k_{f,i}$ whose purpose is to discard the faulty wheel from the torque allocation calculation. The allocation algorithm assigns the torque -which would otherwise be allocated to the faulty one- to the non-faulty wheels.

On the contrary, the *optimal control approach* is an iterative process which tries to minimize the error of a cost function. This allows the engineer to add to this function additional criteria (i.e. constraints) in order to achieve better dynamic behavior. Its main characteristics are the following:

- It is heavy computationally
- It enables the engineer to add other criteria about the force allocation

The aforementioned cost function in its simplest form is presented below.

$$\min g(u) = \min_u \frac{1}{2} \left(||WBTu^{ref} - WF_{veh}^{ref}||_2^2 - \epsilon ||u||_2^2 \right) \quad (2.4)$$

$$F_{veh}^{ref} = BTu^{ref} \quad (2.5)$$

Where matrix B can be seen below and it allocates F_x and M_z to the four non turning wheels and matrix T is the tyre-corner transformation matrix.

$$B = \begin{bmatrix} 1 & 0 & 1 & 0 & 1 & 0 & 1 & 0 \\ 0 & 1 & 0 & 1 & 0 & 1 & 0 & 1 \\ -\frac{s_f}{2} & l_f & \frac{s_f}{2} & l_f & -\frac{s_r}{2} & -l_r & \frac{s_r}{2} & -l_r \end{bmatrix} \quad (2.6)$$

Chapter 3

Initial problem analysis

Before entering the implementation phase, it is important to support the reader with all the basic information which were derived on this thesis and led to the final goals and strategies. Initially, this chapter will present all faults that this project focuses on. Next, the yaw control mechanisms that the RCV is equipped with will be analyzed. This information will provide the background to support the final thesis scope definition. Finally, there is a short description containing the delimitations w.r.t. ISO 26262 in this project.

3.1 Fault consequences

In this sub-chapter, the most severe of the selected faults will be presented in order to assess their consequences during driving. All the measurements presented below are derived from actual tests conducted on the RCV in which the vehicle follows a straight path and the deviation in yaw rate is only caused by the corresponding fault.

Also, in an effort to increase the scientific height of the thesis, additional work has been conducted concerning fail-operational behavior. In that respect, possible sources of unintended yaw rate were investigated and listed, prioritizing failures of on-board systems, for further analysis. These faults are presented in sub-chapter [3.2](#).

3.1.1 Drive shutdown

The drives which are mounted on the RCV have already fault diagnostic mechanisms which (depending on the fault) shut down the drive's power stage, reducing the torque of the corresponding motor to zero to protect it from the consequences of the fault. In figure 3.1 at $t = 152\text{ s}$, the rear left motor shuts down during a test drive at a longitudinal velocity of $v_x = 45\text{ km/h}$.

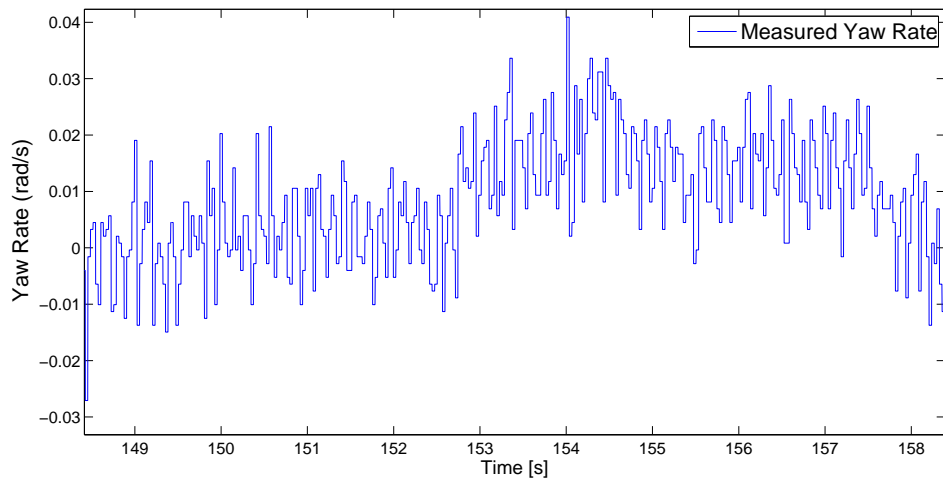


FIGURE 3.1: Measured yaw response of the RCV during motor-drive shutdown

It can be seen that the change in the vehicle's yaw rate caused by the drive shutdown is $0.01 < \Delta\dot{\psi} < 0.02\text{ rad/s}$ which is a negligible change. A more intuitive way to prove that the effects of this fault are easily manageable, is the fact that this fault occurred during tests in the past and the drivers did not notice the difference in yaw rate. Only after the tests were conducted was it realized that one of the motors had shut down. Thus, the analysis of these faults in regards to fault handling was deemed unnecessary.

3.1.2 Inverted torque

A more severe group of faults induce a breaking torque to the wheel which can prove to be dangerous. More specifically, the faults presented here are included in Fault Groups 3, 5 and 6 which can be seen in tables C.1 and C.2. Fault group 3 is composed of faults that can be detected by the motor drives but since their failure

effect can induce high yaw rate on the vehicle's response, it is deemed important to analyze the incident that they will not be detected by the drives' fault diagnostic mechanism. On the contrary, the faults included in fault groups 5 and 6, are faults that cannot be detected and their consequences are unpredictable.

In figure 3.2 the yaw rate response of the vehicle, moving with a longitudinal velocity of $v_x = 33 \text{ km/h}$. At $t = 70 \text{ s}$ a braking torque of 50 Nm was induced in one wheel. Similarly, in figure 3.3 at $t = 198 \text{ s}$ a braking torque of 100 Nm was induced in one wheel while the vehicle had a longitudinal velocity of $v_x = 30 \text{ km/h}$.

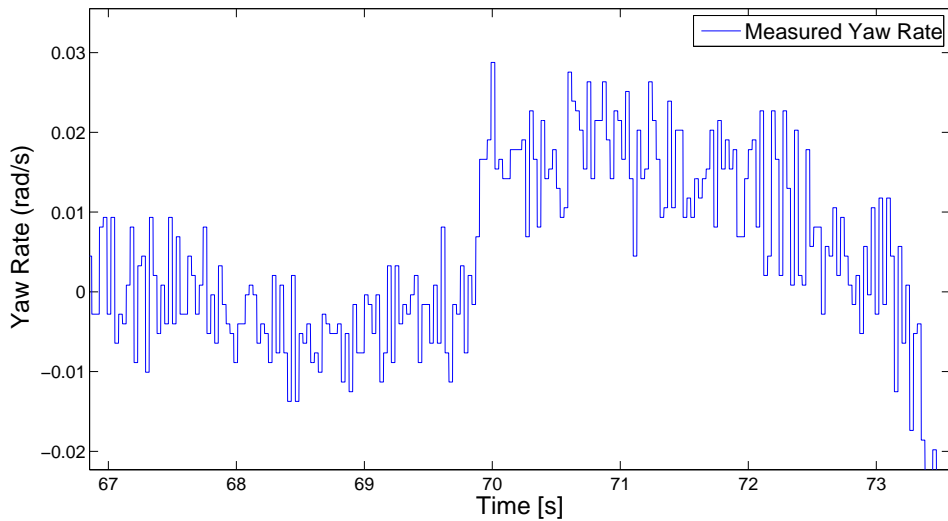


FIGURE 3.2: Measured yaw rate response of the RCV during the induction of 50 Nm breaking torque on rear left wheel

It can be seen that these faults induce noticeable yaw rate divergence at low velocities.

Also, in figures 3.4 and 3.5, the effect that these faults have on the vehicle's longitudinal velocity are presented. More specifically, having a constant torque signal on all motors, while one of the motors is commanded to apply a braking torque on the wheel. There is a noticeable change in the vehicle's velocity. Of course the driver can compensate for that by pushing the throttle but depending on the conditions, that can saturate the motors if the torque allocation scheme is used.

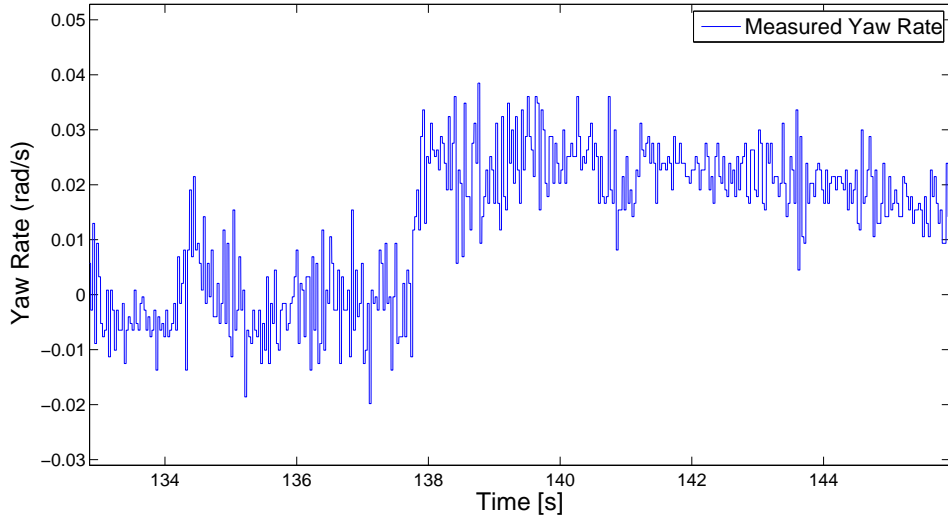


FIGURE 3.3: Measured yaw rate response of the RCV during the induction of 100Nm breaking torque on rear left wheel

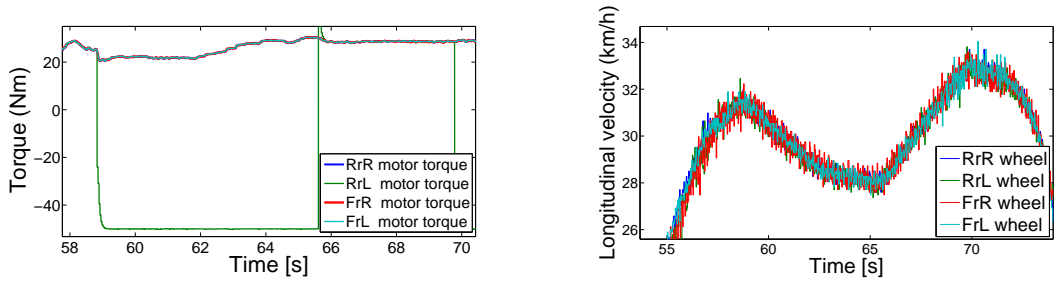


FIGURE 3.4: Measured motor torques (to the left) and wheel velocities (to the right) during the induction of a 50Nm breaking torque on rear left wheel

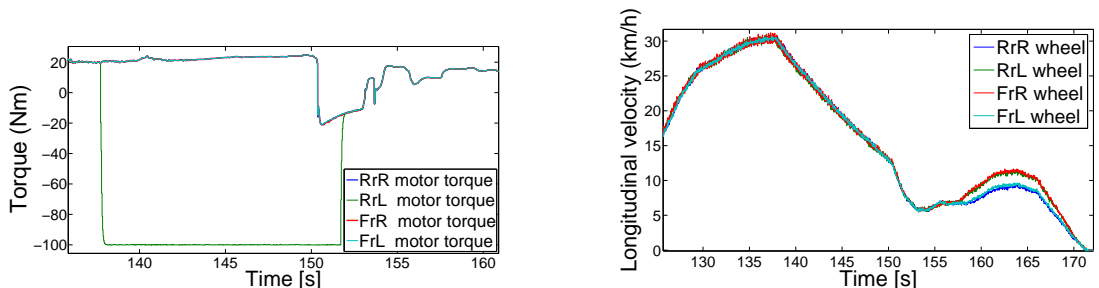


FIGURE 3.5: Measured motor torques (to the left) and wheel velocities (to the right) during the induction of a 100Nm breaking torque on rear left wheel

3.1.3 Wheel lock

The wheel lock fault can be proven extremely dangerous, especially at higher velocities. In figure 3.6, the yaw rate response of the vehicle is presented.

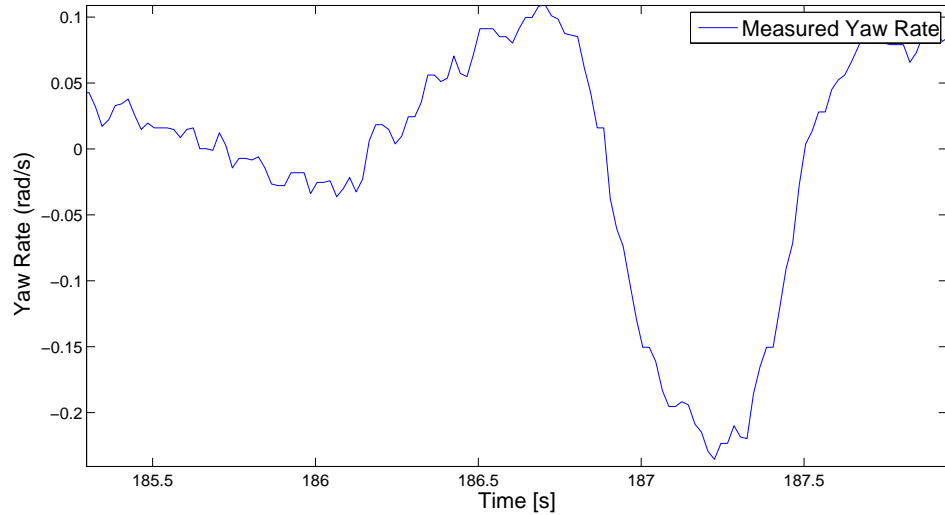


FIGURE 3.6: Measured yaw response of the RCV during wheel lock

At $t = 186\text{ s}$, the rear left wheel is locked and the yaw rate starts increasing. At 186.7 s , the driver makes a correcting maneuver and the measurement cannot show the clear effect of the fault afterwards. This test was conducted at $v_x = 25\text{ km/h}$ longitudinal velocity and it is visible that its consequences can easily lead to the loss of the vehicle's control.

3.2 Additional faults related to fail-operational analysis

In this section, additional faults are presented and analyzed as part of the fail-operational behavior analysis. The failures whose consequences are going to be investigated originate from sensors, actuators, networks and power supplies. The analysis focuses on whether each fault group includes yaw rate on the vehicle's response.

Sensor failure can induce unintended yaw rate in many different ways. Since the failures of the sensors that are mounted in the motor drives are included in

the actuator failure category below, the sensors that will be analyzed here are the IMU-GPS sensors.

IMU failure can result in steering unavailability because if the active steering is enabled, it will try to negate any steering if it diverges from the (faulty) measurement. Unfortunately, the IMU currently used does not support fault diagnosis so as to inform the ECU that its measurements cannot be trusted. Hence, a solution to this problem would be to disable the active steering controller once such a problem is detected. Such a detection algorithm does not exist though and its design is out of this thesis' scope.

Actuator failure. In this group of failures, all the faults that relate to the actuators and their drives are included. Hence, motor drive sensor failures are included here as well. The two groups of actuators whose failure can result in unintended yaw rate induction on the vehicle, are the hub-motors and the steering actuators. The analysis of hub-motor failures was in the immediate goals of this thesis from the beginning. The steering actuator failures though have not been addressed.

In the "EPOS firmware specification" manual [14], the different faults that can be detected are presented and the drives' response is described. As it can be seen in that document, most of the faults described, result in a deactivation of the corresponding actuator or to a "Quick deceleration stop" which is followed by an actuator shut down. Since all the detected faults result in an actuator shut down, the tests carried out to validate fail operational behavior will be limited to steering actuator shut down.

Network failure. In the RCV there exist two CAN networks. The first CAN network is responsible for the transmission of the hub-motor signals to the MicroAutoBox. A possible failure would make the driver unable to accelerate but would not have any effect on the yaw rate response of the vehicle.

Instead, the second CAN network is responsible for the transmission of IMU's, steering wheel and steering actuator's signals to and from the MicroAutoBox. Hence, a possible failure would make the driver unable to steer and thus unable

to control the yaw rate of the vehicle. Since these faults cannot induce yaw rate on the vehicle's response, they will not be studied further.

The **power supply** includes two batteries, the main 48V battery and a 24V auxiliary battery. When the vehicle is operating, the auxiliary battery is charged by the main battery through a DC-DC converter. Hence, a possible failure of the auxiliary battery will not affect the vehicles response. On the contrary, a possible failure of the main battery would result in power loss of all the hub-motors which will immediately shut down. In such a case, the steering abilities are not compromised and the driver can proceed to a safe stop.

Based on the aforementioned analysis and in order to verify the fail-operational behavior of the vehicle, the disabling of one steering actuator was added in the test list. In order to achieve that, the power cable for the actuator is disconnected from the drive.

3.3 Fault selection

As already described in the chapter 1.1, based on an analysis carried out in [4], a set of faults was chosen for further investigation concerning detection and handling. After having analyzed the consequences of the most severe faults in chapter 3.1 and having conducted an analysis on failures that can arise in the vehicle's on-board systems, a more concrete list of the faults that this thesis is going to focus on is presented in table 3.1.

TABLE 3.1: A table consisting the faults that are going to be further analyzed concerning fault handling

Faults	Failure effect	Fault description
FG 3	Braking torque	Short circuit
FG 5	Wheel lock	Destruction of turning parts
FG 6	Braking torque	Sensor failure
Steering actuator faults	One wheel not steering	Steering actuator deactivation

Based on table 3.1, the cases that need to be tested are the following:

- Braking torque

- Wheel lock
- Steering actuator deactivation

In order to get a good representation of the faults without actually damaging the vehicle, all the faults will be artificially induced. More information on this topic can be found in chapter [4.1.2](#).

3.4 Yaw rate control mechanisms

In order to design an efficient fault tolerant controller, all the possible yaw rate control mechanisms had to be studied. The two main mechanisms are the torque allocation and the active steering approaches. As can be seen in [\[1\]](#), a torque allocation technique has already been implemented which shows encouraging results towards fault compensation. Despite that, this controller can only have limited results since the motors are responsible for the longitudinal velocity of the vehicle (which should be maintained if possible in case of faulty conditions) and can have limited effect on the yaw rate response of the vehicle since they need significantly more control effort compared to the steering system in order to have the same results. Hence, the motors tend to saturate in the most severe faults or on higher velocities.

Despite that, the torque allocation approach has a major advantage over the steering control, which is the response time. The steering actuators currently used on the RCV have a significant time delay which can be seen in figure [4.4](#) where a step response of the steering actuators is presented. On the contrary, the motors have a small time delay until they build up the current necessary for the required torque.

The steering controllers on the other hand, although being slower than the hub-motors, are more efficient at controlling yaw rate. All these aforementioned characteristics will be used for the definition of the fault tolerant controller in the next chapter.

3.5 Active steering

Given that an active steering approach was very appealing for fault tolerant control, a lot of literature concerning the implementation of an active steering controller was found and studied. In [15], the use of a sliding mode controller is introduced for robustness on model uncertainties. In many publications like [16], [17] and [18], there are analytical explanations of sliding mode controllers and their functionality. It is important to be noted here, that control approaches using optimal control or quadratic programming were rejected since they are computational heavy and cannot be implemented in the current system configuration. Finally, although the aforementioned literature was studied, a simpler PI controller was adopted for the active steering controller since the remaining time to implement the controller was limited and the experience in nonlinear control was limited at the time.

3.6 Fault handling approaches and change of scope

After analyzing the work that has been carried out previously on this topic and more specifically on the RCV, a valid conclusion is that there is extensive research interest in the implementation of active steering controllers which can prove to be very efficient for fault compensation. Such a system has not been studied yet for the RCV. Hence and after analyzing the delimitations in chapter 1.3, the main interest of this thesis was shifted from the use of safety standards and fault detection, to the implementation of an active steering fault tolerant controller. In figure 3.7 it can be seen how the initial fault compensation setup evolved to become an active steering with the ability to be combined with the existing torque allocation scheme.

In faulty conditions, fast compensation response is crucial for both safety and driving comfort. Hence and given the analysis in 3.4, the goal of this thesis on the control level, is to implement a steering controller, able to collaborate with the torque allocation controller which will provide fault compensation by harnessing

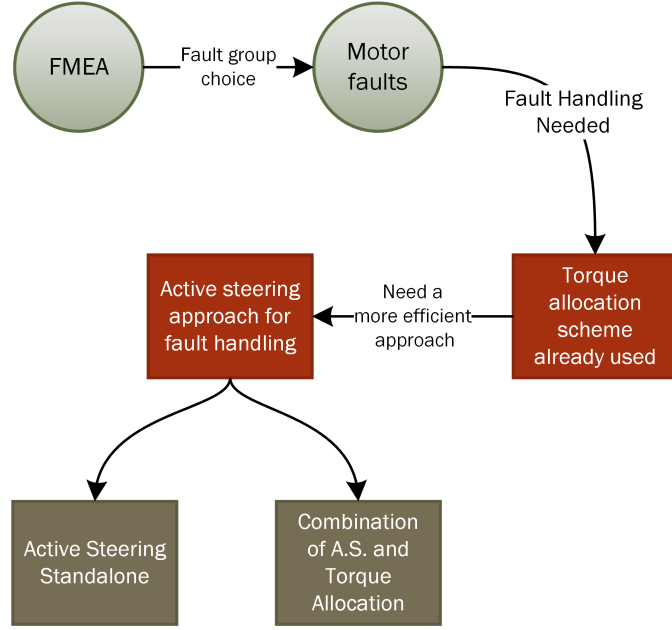


FIGURE 3.7: Thesis fault handling approach

the advantages of both techniques. More specifically, the proposed approaches for fault handling are the following:

1. Steering controller standalone
2. Steering controller and torque allocation working in parallel
3. Steering controller and torque allocation working in parallel, with the additional integration of torque allocation's control signal in the steering controller (presented in chapter 4.4.2).

Finally, as was analyzed in 3.1, the faults that need to be compensated are mainly faults that cannot be detected by the drives. Thus, the purpose of the steering controller was changed from a fault activated system to a continuously active system which enforces the vehicle to follow the reference yaw rate at all times.

3.7 ISO 26262 delimitations

One major aspect of this thesis is safety which is mainly comprised of the use of ISO standard 26262 for the definition of ASIL levels on the different hazards.

ISO 26262 is a standard which refers to all the stages of the production of a conventional vehicle. Since RCV is a prototype and many of the ISO's guidelines cannot be implemented, it was initially believed that it would help since it provides a structured methodology as well as useful tools to work with.

Instead, it was realized that since the RCV was already built, the motor drives were complex systems which could be handled only as black boxes and the addition of hardware for the fulfillment of the requirements set in the previous stages of the ISO 26262 was deemed out of the thesis scope; the extent at which the standard could be used was quite limited. Hence, the only topic that was implemented was the ASIL level assignment.

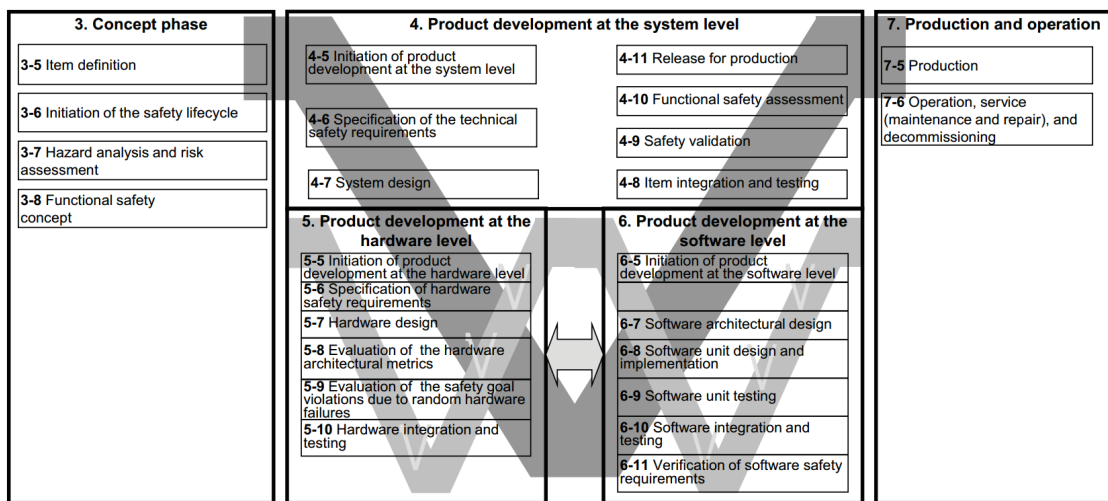


FIGURE 3.8: V model overview of ISO 26262

In figure 3.8, the V-model overview of ISO 26262 is presented. The thesis started at step "3. Concept phase" where the ASIL level assignment was carried out (which is presented in chapter 4.2), and a draft "Item definition" and "Functional Safety Concept" was derived.

Next step was "4. Product development at the system level". After getting acquainted with this chapter of ISO 26262, some initial work was carried out, while simultaneously the different fault detection mechanisms were examined for the specific fault group. During this examination, it was realized that a big group of faults was already diagnosed by the motor driver. Hence, the following step was to explore what possible ways existed to detect all the selected faults by exploiting hardware and software means leading this way to ISO 26262 steps 5 and 6. At

At this point, different detection mechanisms were investigated. Such mechanisms included the addition of sensors outside of the motor drives in order to cover redundancy issues as suggested in ISO 26262, as well as the addition of software mechanisms including comparison among the wheels' speeds and motors' torques to identify possible faults. Despite that, it was realized that superficial addition and intervention on the motor drive mechanisms was unnecessary and outside of the thesis' scope. Instead, a set of requirements for future choice of motor drives will be presented in chapter 7.2.

Following this conclusion, in terms of ISO utility in this thesis, the work was mainly directed to step "6. Product development at the software level". Here, a set of guidelines is introduced for compliance with ISO 26262 which can be seen in table 3.2. For this purpose, and given that the software is implemented in Simulink and flashed on a MicroAutoBox, a book titled "Modeling Guidelines for MATLAB/Simulink/Stateflow and TargetLink" ([19]) was studied which entails all the useful information.

Topics	ASIL			
	A	B	C	D
1a Enforcement of low complexity ^a	++	++	++	++
1b Use of language subsets ^b	++	++	++	++
1c Enforcement of strong typing ^c	++	++	++	++
1d Use of defensive implementation techniques	o	+	++	++
1e Use of established design principles	+	+	+	++
1f Use of unambiguous graphical representation	+	++	++	++
1g Use of style guides	+	++	++	++
1h Use of naming conventions	++	++	++	++

TABLE 3.2: ISO 26262 coding and modeling guidelines

Although this part of ISO 26262 could be implemented, the magnitude of the dSPACE model is big and would require time to implement. As an alternative, there was the suggestion of implementing these guidelines only in the steering controller block which would be designed for this thesis, but that would have no impact on the vehicle safety-wise and was deemed unnecessary.

Chapter 4

Implementation

In this chapter, all the implementation stages are presented. More specifically, it is divided into practical implementation, ASIL assignment, modeling and control implementation sections.

4.1 Practical implementation

The experimental validation of the fault tolerant controller demanded a fully functional vehicle, on which the analyzed faults would be induced. The main focus of this sub-chapter, is to describe all the parts that were added on the RCV in order to make it possible to implement fault handling algorithms.

4.1.1 IMU installation

Another factor that required time to set up was the IMU-GPS system which was decided to be replaced. The new package is produced by Racelogic and it is comprised of an IMU unit which is mounted on the vehicle's CoG and a dual antenna GPS system which is mounted on the roof of the vehicle (one antenna on each side) as can be seen in figure 4.3. The IMU is not visible because it is mounted between the two chairs of the vehicle where the CoG is located. After mounting them, some calibration through the VBOX software was needed as well

as some changes in the Simulink model in order to be adjusted for the new units to be ready for use.

The IMU unit is going to provide to the fault compensation controllers the information of yaw rate and lateral acceleration which are required for their function. The GPS unit is needed for two reasons; firstly because the system correlates the GPS data with those acquired from the IMU to derive more accurate measurements and secondly, because the RCV is also used in autonomous driving mode.

Unfortunately, a series of problems arose during the setup of the IMU. More specifically, after some initial test-drives were conducted on the RCV, it was realized that the IMU data is delayed by approximately $400ms$ which would have a serious negative effect on the controllers. Hence, the solution to this problem was prioritized. After testing, it was realized that the calibration of the GPS was the reason for this delay. Hence, the GPS antennas were disconnected for the purposes of this thesis.

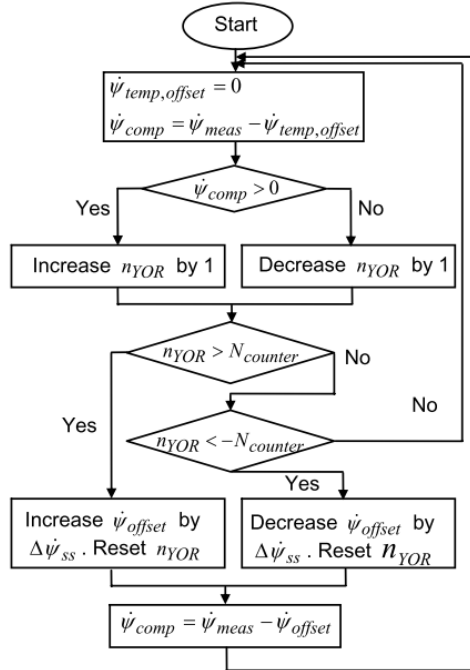


FIGURE 4.1: Functional flow chart of the dynamic DC offset compensation algorithm

One major problem that arises during the vehicle's motion, is that there is a lot of vibrations due to the road profile which induce a lot of noise in the IMU's measurement that affect the controller's functionality. In order to avoid this behavior,

the IMU is mounted on a foam base in order to dissipate some of the vibrations.

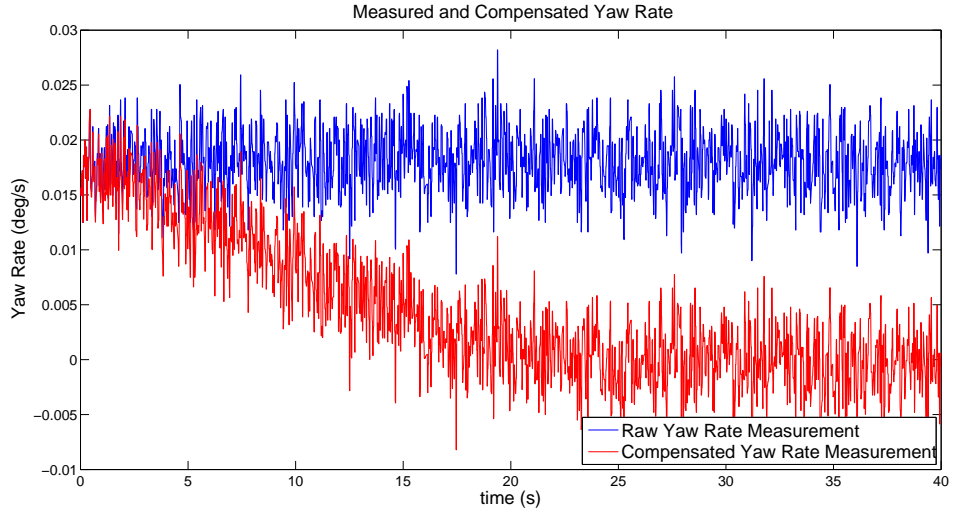


FIGURE 4.2: Compensation of DC offset using the sequential compensation algorithm

Also, since the controller used for the active steering is a PI, the gyro's dynamic offset has a negative impact on its integral part. Hence, a dynamic offset algorithm presented in [20] whose functional flow chart can be seen in figure 4.1, was implemented. In figure 4.2, an example of measurement compensation is presented where in order to have a more visible difference between the two signals, an additional offset of $c_{offset} = 0.02 \text{ deg/s}$ was added on the measured data. The convergence time and the accuracy of the compensator depends on the $\Delta\dot{\psi}_{ss}$ value. Choosing a bigger $\Delta\dot{\psi}_{ss}$ decreases the convergence time but decreases also the accuracy. Normally, $0.001 < \dot{\psi}_{offset} < 0.002 \text{ deg/s}$, which is a rather small value on which the compensator can diverge quickly and be accurate. It is possible to improve the compensator's behavior by adding a dynamic $\Delta\dot{\psi}_{ss}$ calculator but such a thing is not necessary for this thesis since the compensator converges in $t < 3 \text{ s}$. Finally, the sequential algorithm calibrates the DC offset value only while $\delta < 0.001 \text{ rad}$ or $v_x < 0.1 \text{ km/s}$.

4.1.2 Fault induction setup

A final part of the practical implementation on the RCV is the setup of the fault induction mechanisms. The faults that are going to be tested are: braking torque on one wheel, lock of one wheel and deactivation of one steering actuator.



FIGURE 4.3: GPS antennas and IMU placement

The induction of **braking torque** was implemented using software. More specifically, a change in the torque reference value was used which was activated through the joystick that the co-driver uses for safety reasons.

The **wheel lock** fault was induced through a handbrake which controlled the brake of the rear left wheel and was activated by the driver.

The **deactivation of a steering actuator** is the final test that was carried out in the RCV. In order to deactivate the steering actuator, its power supply was disconnected before the test.

4.2 ASIL assignment

For the purposes of this process, the different faults were divided in categories based on their failure effects. Since many of the failure effects of the faults did not have major impact on the vehicle's behavior, they were disregarded. More specifically, the 4 categories that were studied include the faults which have the following failure effects:

- 100% torque loss on one wheel
- 25% torque inversion
- 40% torque inversion

- high breaking torque reaching up to 400N

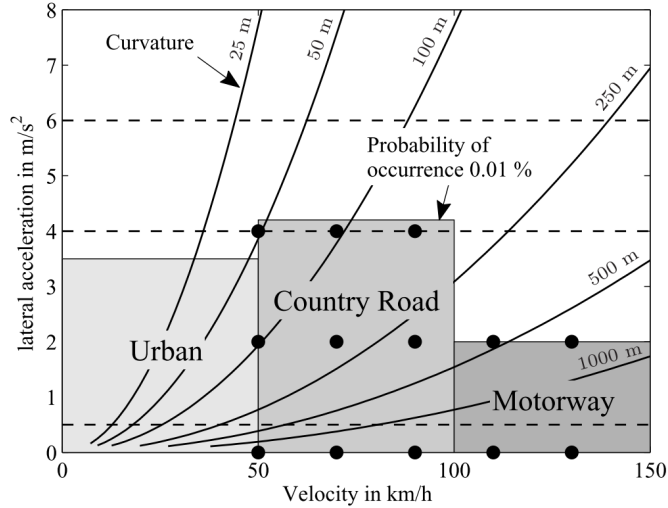


TABLE 4.1: Areas of lateral acceleration for normal driving

In figure 4.1 which was taken from [4], the lateral acceleration for 99.99% of the normal driving behavior is mapped. Based on this analysis and since the RCV cannot exceed velocities of 55 km/h, the decided driving environments were chosen based on the factors that can affect the faults occurrence positively. The driving behavior under which the corresponding ASIL levels were derived were:

- for a longitudinal velocity of 25 km/h, lateral acceleration of 0 m/s^2 , 1.5 m/s^2 and 3 m/s^2
- for a longitudinal velocity of 50 km/h, lateral acceleration of 0 m/s^2 , 1.5 m/s^2 and 3 m/s^2

In order to introduce more objective criteria on the derivation of the different ASIL levels, a technique used in [4] was implemented for the controllability ranking. More specifically, controllability is divided in the following four classes:

- C0 - controllable
- C1 - easy to control
- C2 - difficult to control

- C3 - uncontrollable

The level of controllability is determined based on 3 indexes:

1. Q_z - vehicle stability index
2. Q_y - lane keeping index
3. Q_x - collision avoidance index

These indexes are derived by mathematical equations and are further analyzed in [4]. Based on these criteria for controllability and on the description of severity and probability indexes in the ISO 26262 documentation, table 4.2 was derived which includes the ASIL levels for the most severe faults.

4.3 Modeling

This section presents an analysis on the modeling aspects of this thesis. The three main aspects of modeling correspond to the steering actuator model identification, the parameter tuning process of a bicycle model and the parameter tuning process of a complex vehicle model. It is important to be noted here, that the two main reasons why this tuning effort was deemed necessary, were safety during testing and RCV's availability issues that arose in the beginning of this thesis. During testing of the controllers, in order to avoid any damage to the vehicle or even injury, the controllers need to be as close to reality as possible.

4.3.1 Steering actuators

As already mentioned, the RCV is comprised of 4 steering actuators. The EPOS 70/10 are the motor controllers that are used to drive these four linear actuators and they are set in position mode. The reference position of the linear actuators is sent from the MicroAutoBox through CAN.

Failure effect	Driving Environment and Driving Behavior		Severity	Probability	Qx	Qy	Qz	Q	ASIL
100 % reduction	Residential areas with 30km/h speed limit, bumpy road, icy road	25 km/h 0 m/s^2	S0	E4	0.1	>5	0.1	C0	QM
		25 km/h 1.5 m/s^2	S1	E3	0.2	>5	2	C0	QM
		25 km/h 3 m/s^2	S1	E1	0.3	4.8	4.8	C2	QM
	City-drive 50 km/h, bumpy road, icy road	50 km/h 0 m/s^2	S2	E4	0	>5	0.7	C0	QM
		50 km/h 1.5 m/s^2	S2	E3	0.3	>5	3	C1	QM
		50 km/h 3 m/s^2	S3	E1	0.5	3.1	4	C3	QM
25 % inverted torque	Residential areas with 30km/h speed limit, bumpy road	25 km/h 0 m/s^2	S0	E4	0.1	>5	0.5	C0	QM
		25 km/h 1.5 m/s^2	S1	E3	0.5	>5	3.5	C1	QM
		25 km/h 3 m/s^2	S1	E1	0.6	5	6	C3	QM
	City-drive 50 km/h, bumpy road	50 km/h 0 m/s^2	S2	E4	0	>5	1.2	C0	QM
		50 km/h 1.5 m/s^2	S2	E3	0.5	3.6	3.8	C2	QM
		50 km/h 3 m/s^2	S3	E1	0.5	3.4	6	C3	QM
40 % inverted torque	Residential areas with 30km/h speed limit, bumpy road	25 km/h 0 m/s^2	S0	E4	0	>5	0.4	C0	QM
		25 km/h 1.5 m/s^2	S1	E3	0.5	4.8	3	C1	QM
		25 km/h 3 m/s^2	S1	E1	0.7	3.4	6.5	C3	QM
	City-drive 50 km/h, bumpy road	50 km/h 0 m/s^2	S2	E4	0.1	>5	1	C0	QM
		50 km/h 1.5 m/s^2	S2	E3	0.5	3	3.3	C2	ASIL A
		50 km/h 3 m/s^2	S3	E1	1	2.8	8	C3	ASIL A
High breaking torque	Residential areas with 30km/h speed limit, bumpy road	25 km/h 0 m/s^2	S0	E4	3.5.	1.7	2	C3	QM
		25 km/h 1.5 m/s^2	S1	E3	4	1.8	13	C3	ASIL A
		25 km/h 3 m/s^2	S1	E1	4.7	1.6	16	C3	QM
	City-drive 50 km/h, bumpy road	50 km/h 0 m/s^2	S2	E4	3.5	1.7	15	C3	ASIL C
		50 km/h 1.5 m/s^2	S2	E3	4.5	1.6	18	C3	ASIL B
		50 km/h 3 m/s^2	S3	E1	5	1.5	23	C3	ASIL A

TABLE 4.2: ASIL level derivation table

Since the response of the actuators is one of the most important factors that affect the vehicles response and one of the proposed techniques for fault handling is through an active steering approach, it was deemed important to create a model that would fit their response up to an acceptable level.

$$G = \frac{0.0328z}{z - 0.9744} \quad \Delta t = 2 \text{ ms} \quad (4.1)$$

In order to create a model, Matlab's System Identification toolbox was used. The data used for the tuning was a step input on the steering wheel. The result of this process is a discrete transfer function presented in 4.1. Also, in figures 4.4, the step responses of the real and simulated systems are presented.

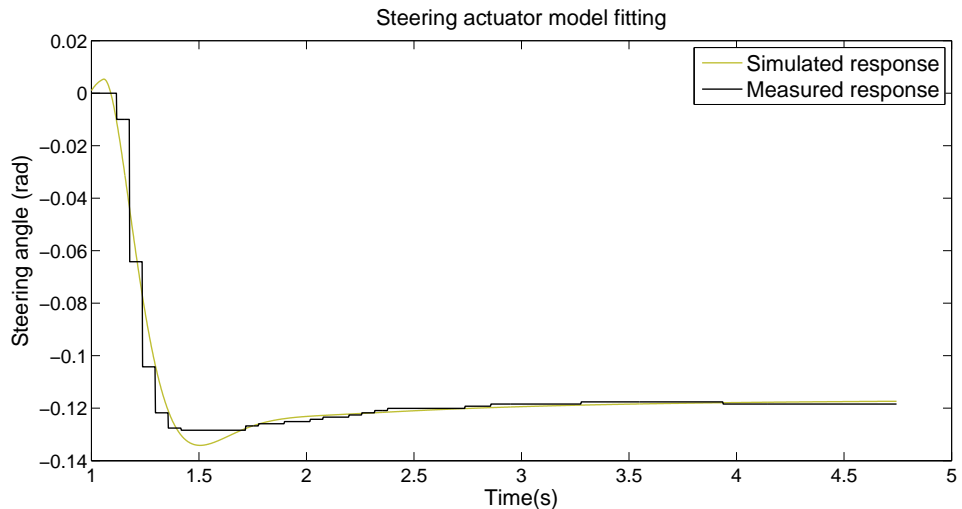


FIGURE 4.4: Fitting of the steering actuator model

Finally, the validation of the derived steering model can be seen in figure 4.5. Although not perfectly fitted, the response of the derived model is deemed adequate for the purposes of this thesis.

4.3.2 Bicycle model

For the implementation of a fault handling strategy, a reference creating mechanism is needed for the controllers to follow. In the case of the RCV, that mechanism is the *Bicycle model* which derives the yaw rate reference. The bicycle model can be seen in figure 4.6 and its behavior is described by the differential equation 4.2.

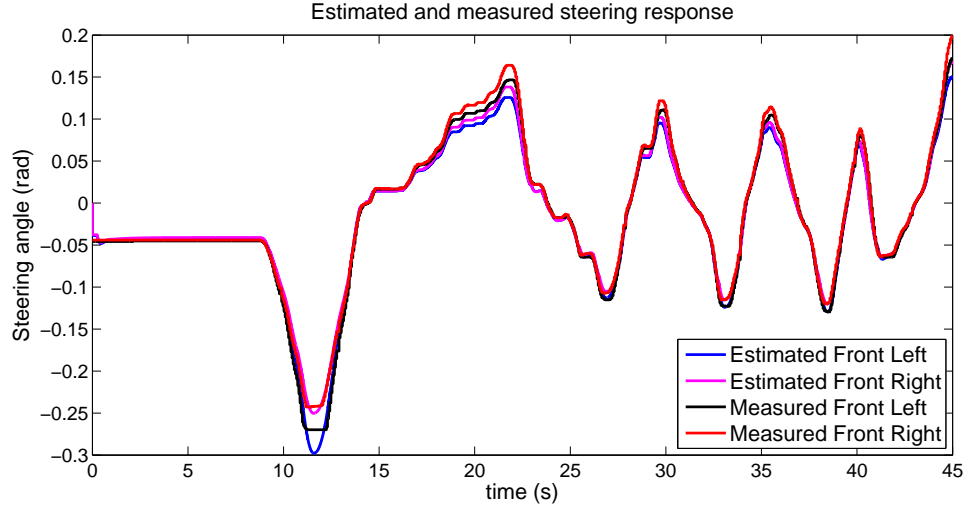


FIGURE 4.5: Validation of the steering actuator model

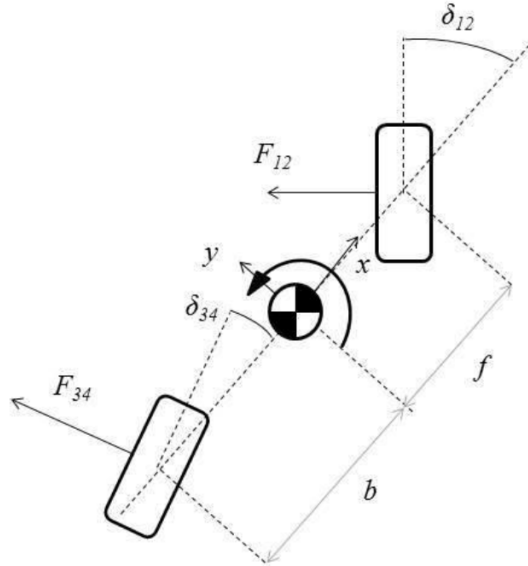


FIGURE 4.6: Bicycle model

$$\begin{bmatrix} mD + \frac{C_{12}+C_{34}}{v_x} & mv_x + \frac{fC_{12}-bC_{34}}{v_x} \\ \frac{fC_{12}-bC_{34}}{v_x} & JD + \frac{f^2C_{12}+b^2C_{34}}{v_x} \end{bmatrix} \begin{bmatrix} v_y \\ \dot{\psi} \end{bmatrix} = \begin{bmatrix} C_{12} \\ fC_{12} \end{bmatrix} \delta_{12} + \begin{bmatrix} C_{34} \\ bC_{34} \end{bmatrix} \delta_{34} \quad (4.2)$$

Where, m is the vehicle's mass, C_{12} and C_{34} are the tire stiffnesses, v_x the longitudinal velocity, v_y is the lateral velocity, $\dot{\psi}$ is the yaw rate, δ_{12} and δ_{34} are the steering angles in the front and back wheels respectively and D is the derivative term.

Currently, the bicycle model is used only under faulty conditions, when the fault compensating controller is activated. Its job is to provide to the controllers, a trajectory that the vehicle would follow without the fault. Thus, it is important that the bicycle model follows closely the vehicle's response because if that is not the case, undesirable transient responses will show up additional to the faulty conditions. More specifically, during the occurrence of a faulty condition, the behavior of the vehicle would change according to the reference derived from the bicycle model. Such a case, would add more tension to the driver and could lead to loss of the vehicle's control. Hence, the tuning of the bicycle model was deemed very important.

The tuning was implemented using the parameter estimation toolbox in Matlab. The tuned parameters were: C_{12} and C_{34} . After this process, a gain block was added on the yaw rate whose value is determined by a lookup table.

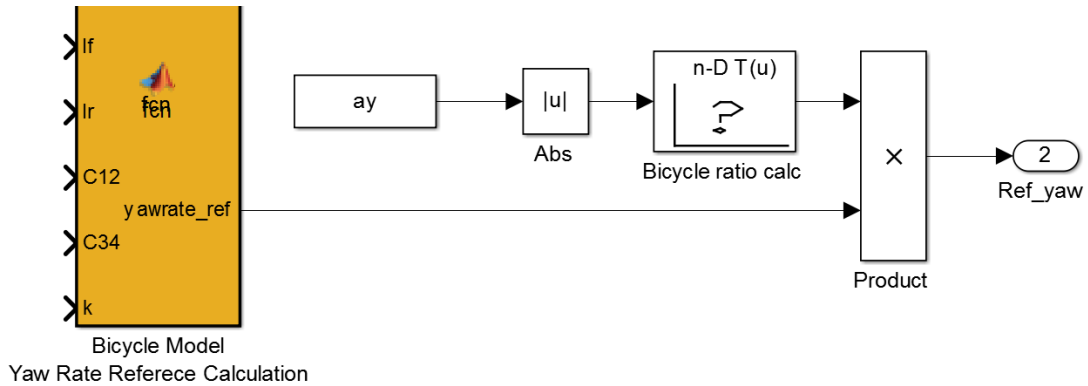


FIGURE 4.7: Bicycle look-up table Simulink diagram

As can be seen in figure 4.7, "yawrate_ref" signal which is an output of the bicycle model block is multiplied by a ratio whose value is derived from the 1-D look-up table "Bicycle ratio calc". The measured lateral acceleration is the input to this look-up table and according to this measurement, the yaw rate gain value is determined. In matrices 4.3 and 4.4, the values of lateral acceleration are coupled with the yaw rate gain values. The first row in matrix 4.4 includes the gain values for 2WS mode while the second row includes the values for the currently used 4WS mode which allocates the steering of the front and rear wheels equally.

$$a_y = [0.5 \ 1 \ 1.5 \ 2 \ 3 \ 4 \ 5 \ 7] \quad (4.3)$$

$$gain\ value = \begin{bmatrix} 0.8 & 0.83 & 1.05 & 1 & 1 & 0.95 & 1 & 1.1 \\ 0.75 & 0.8 & 0.85 & 0.85 & 0.85 & 0.85 & 0.9 & 1 \end{bmatrix} \quad (4.4)$$

The result of this tuning process can be seen in figures 4.8 and 4.9, where the estimated data is compared to the measured response data. The estimated values are very close to the vehicle's response which will enable the vehicle to have smooth driving experience and safer fault compensation. Finally, it is important to be noted, that this model accepts the longitudinal velocity and the steering angle as measured inputs which makes it far easier to tune and far less complex a model than a complete vehicle model.

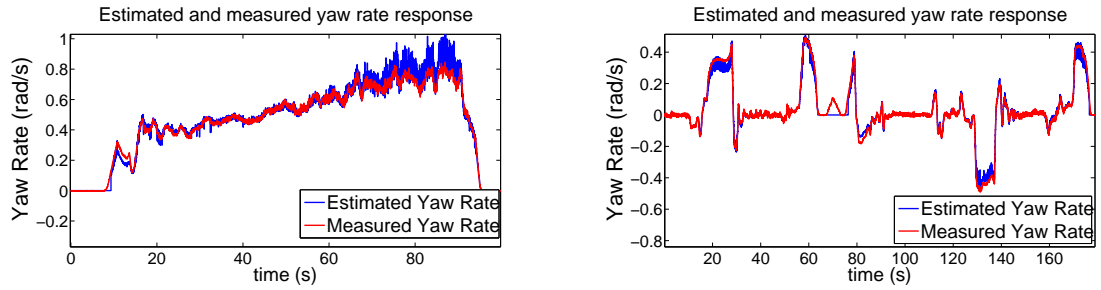


FIGURE 4.8: A bicycle model validation test with constant steering and increasing velocity is conducted (to the left) and a test with induced faults during driving (to the right)

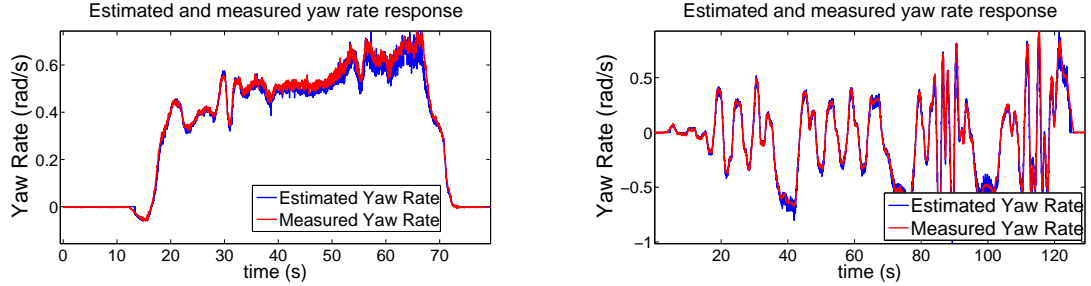


FIGURE 4.9: A bicycle model validation test with constant steering and increasing velocity is conducted (to the left) and a test with slalom driving maneuvers (to the right)

4.3.3 Vehicle model

Although the bicycle model presents a very intriguing way to model the vehicle (at least in terms of yaw rate response), the need for a vehicle model which would describe the behavior of the system in faulty conditions was needed. As can be

seen in equation 4.2, the bicycle model, cannot describe the complex dynamics of a vehicle during faulty conditions, since there is no mention of independent wheel torques and velocities which is where a fault would show up. Hence, a need for such a model arose which would allow the implementation of a controller for fault compensation.

Such a model was derived before the start of this thesis and the goal was to tune this model in order to be a good representation of the real system. Again, Matlab's parameter estimation toolbox was used and the tuning process included more than 10 parameters which increased the complexity and the time needed for this process. These parameters are the following:

- inertias around x,y and z axis
- tire stiffnesses
- l_r, l_f, s_r (see figure 2.1)
- roll resistance
- drag coefficient

Other major challenges towards a tuned vehicle model were:

1. limited knowledge on vehicle dynamics
2. absence during acquisition of the logged data
3. lack of knowledge about the track's profile and slope
4. lack of knowledge about the exact conditions of the vehicle between the different tests.

Finally, the main parameters of interest proved to be, the rolling resistance (f_r), a gain factor applied on the air resistance which was added to the model, as well as a homing compensation parameter that would compensate for any steering misalignment of the wheels during homing of the steering actuators.

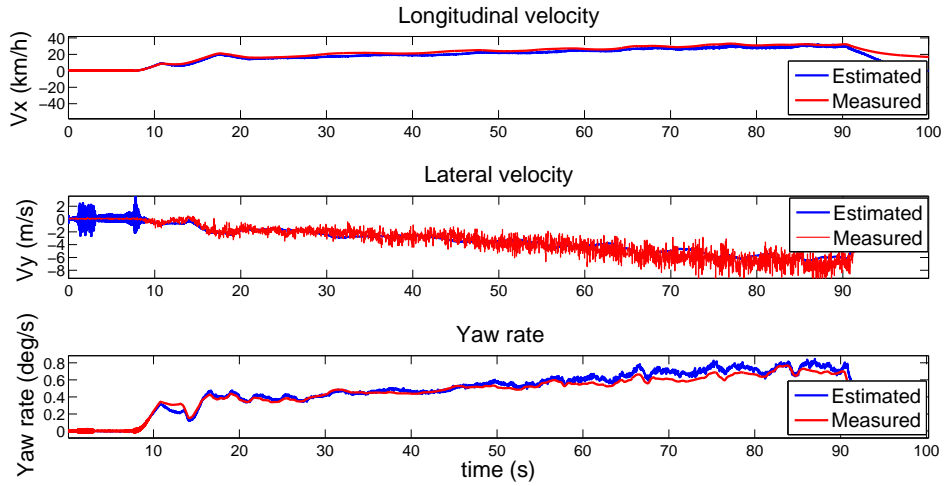


FIGURE 4.10: Constant steering increasing velocity test

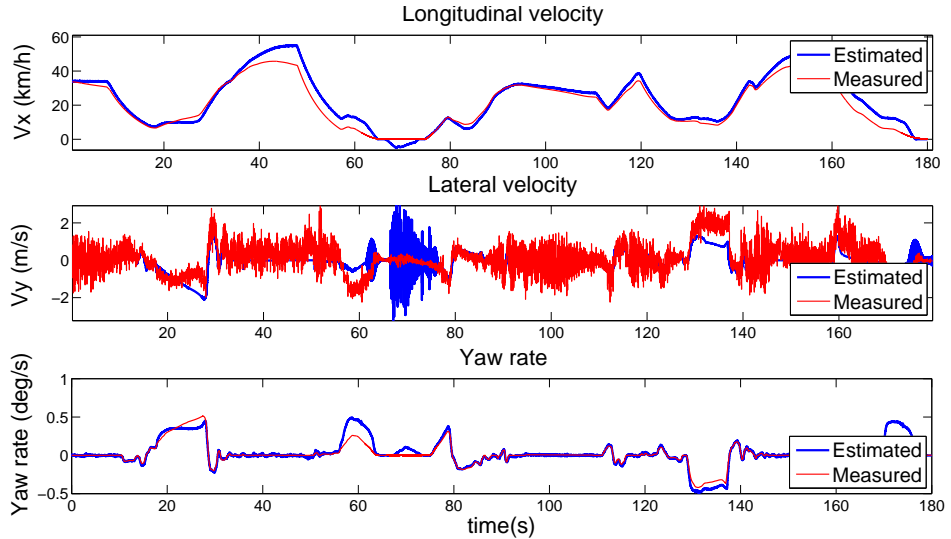


FIGURE 4.11: Model validation on a test case with motor shut down fault induced on the vehicle.

The response of the tuned model compared to the measurements is presented in figures 4.10, 4.11 and 4.12. Despite the fact that a model is difficult to imitate perfectly the response of a physical system, it is important to be noted here that the main reason for inaccuracy in the model's response is the environmental uncertainties. More specifically, the model cannot represent dynamics that are caused by the wind or by the ground inclination. Although not a perfect match, the tuned model is deemed adequate for the scope of this thesis and it will be used for the implementation of the fault compensating controllers.

In figure 4.12, a braking torque of 10 Nm , 50 Nm and 100 Nm is induced on

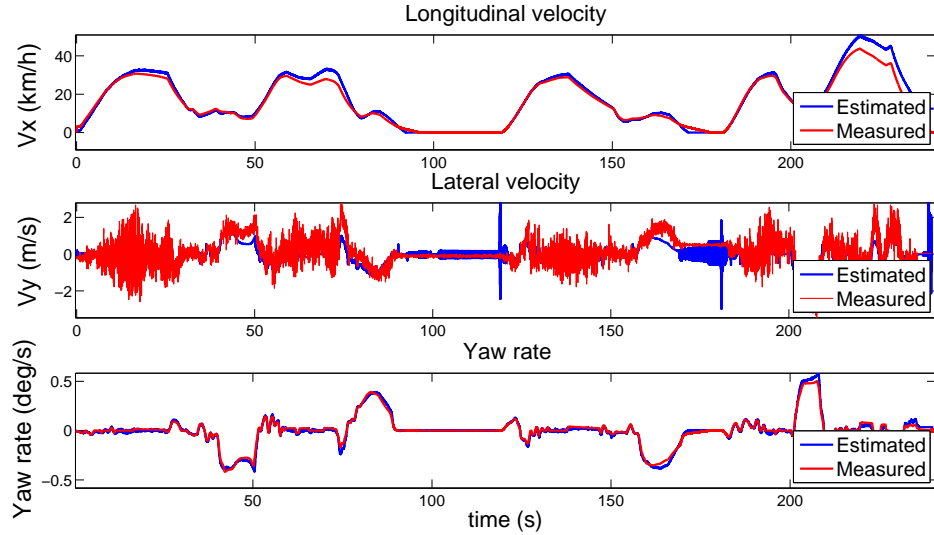


FIGURE 4.12: Model validation on test case with braking torque fault induced on the vehicle.

one wheel at $t = 16, 59, 138\text{ s}$, respectively. In order to get a better view of the model's response in faulty conditions, figure 4.13 is presented which includes the model's response when a braking torque of 100 Nm is introduced on one wheel for $138 < t < 152\text{ s}$. It can be seen here, that the model has a response close to the measured response and is deemed adequate for this thesis.

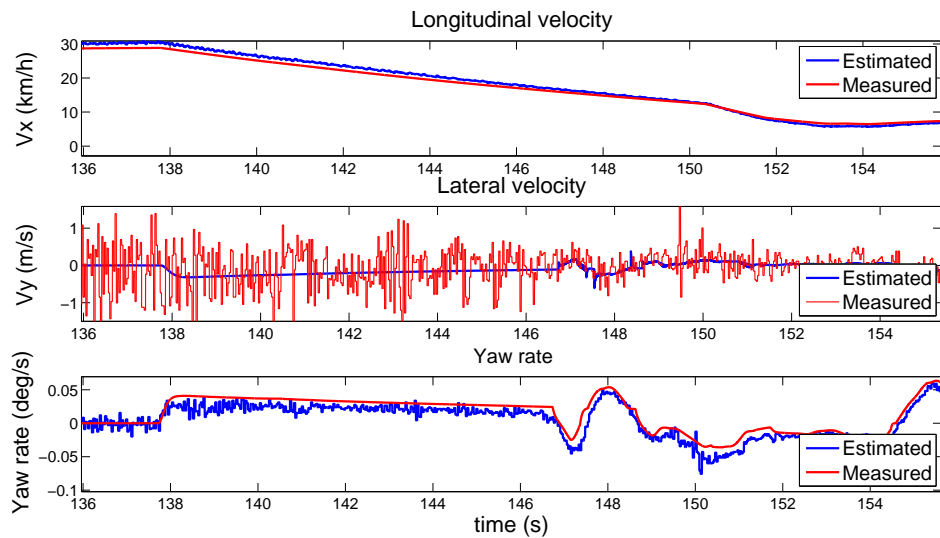


FIGURE 4.13: Model validation on test case with braking torque fault induced on the vehicle, showing faulty condition behavior.

4.3.4 Model

In order to design a steering controller, all these aforementioned tuned models needed to be incorporated into a single Simulink model. In figure 4.14, the structure of this Simulink model is presented.

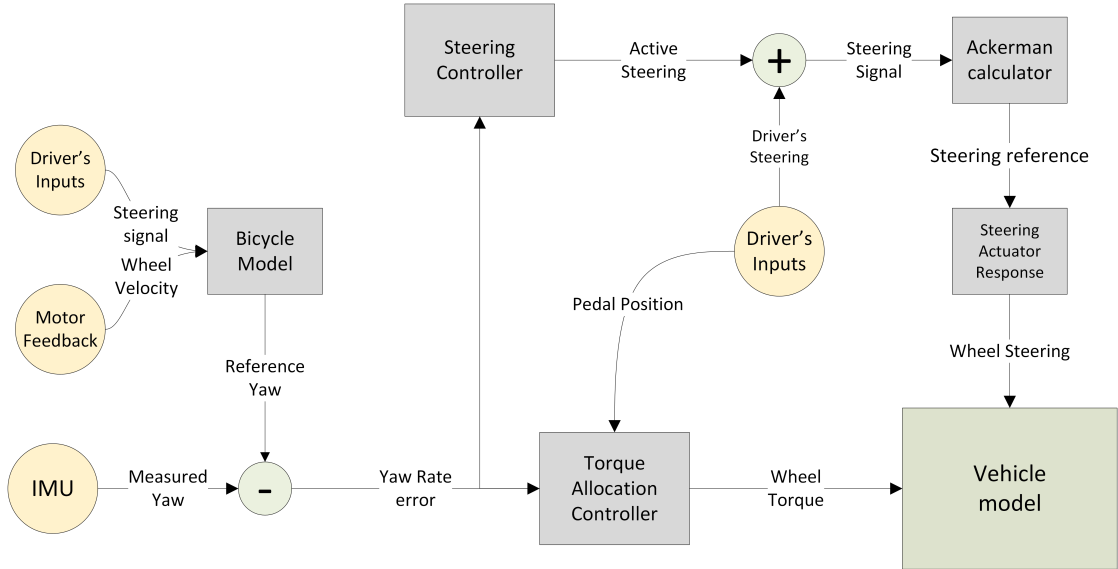


FIGURE 4.14: Complete Simulink model diagram

More specifically, the model is comprised of:

1. the "Driver's input" block which includes the steering signal and the throttle position signal.
2. the "IMU" block, which in the model is the state feedback of the vehicle model and provides the controllers with the vehicle's yaw rate and lateral acceleration.
3. "Steering actuator response", "Bicycle model" and "Vehicle model" blocks which have been already discussed in sections 4.3.1, 4.3.2 and 4.3.3 respectively.
4. the "Steering controller" block which entails the fault tolerant controller and will be explained in section 4.4.2
5. the "Torque allocation controller" block whose function is explained in 2.2

6. and finally, the "Ackerman calculator" block which allocates the steering signal to the steering actuators according to the Ackermann geometry.

4.4 Control

4.4.1 Controller design criteria

In order to implement a fault tolerant controller which will minimize the exposure risk during faulty conditions, a set of criteria need to be set, on which the controller's design will be based. The criteria are:

1. minimization of yaw rate divergence based on driver's reaction time
2. actuation delays smaller than 200 ms
3. the ability to maintain longitudinal vehicle velocity

The actuation delay limit was chosen based on simulation results. During those tests, faults were induced for longitudinal velocities $v_x < 50\text{ km/h}$. It was concluded, that the system would not be able to minimize the yaw rate divergence faster than the driver's reaction time, if the steering actuators had a time constant larger than 200 ms .

Driver's reaction time, is an important parameter for the design of the controller, since it is the time spent until the driver reacts to a fault. Compared to the human driver, since the fault's consequences on the vehicle's response can be detected immediately, the fault tolerant controller loses only a small time interval until it reacts to the fault which is one major advantage.

The reaction time is comprised of three factors, namely the mental processing, movement time and device response time. In [4] there is an extended survey on different publications on this topic. Since this thesis is researching real condition driving, it is rational to assume that the chance of any driver knowing that a fault is imminent is very slim. Hence, the reaction time (t_{rt}) that is going to be adopted here is $1\text{ s} < t_{rt} < 1.25\text{ s}$. During that time, the driver is assumed to be

idle concerning the fault and the goal is to ***reduce the yaw rate error*** during that time to an acceptable low level which will be easier for the driver to handle.

The actuation delay in RCV is comprised of three parts:

1. the measurement delay (derived from the IMU's datasheet [21]) which should be below 8 ms , hence negligible
2. the time to transfer the error signal to the MiniAutoBox through CAN which is below 1 ms and hence negligible
3. the cycle time of the ECU's control algorithms is set to 30 ms
4. time constant in the motors ($t_{90\%} < 50\text{ ms}$), derived from logged data
5. time constant of the steering actuators ($110 < t_{90\%} < 120\text{ ms}$) and is derived from the steering actuator step response presented in figure 4.5.

As a result, the torque allocation approach has a worst case scenario (WCS) delay of 80 ms and the steering controller has a WCS delay of 150 ms .

Maintain longitudinal velocity. Lastly, it is important that the vehicle is able to maintain its velocity during faulty conditions. The fulfillment of this criteria is mainly restricted by the longitudinal force that the motors can provide, the vertical force on each wheel and the force allocation controller which by trying to minimize the yaw rate error, may loose the ability to keep a certain velocity. The latter can happen when the torque allocation controller saturates the hub-motors. Hence, this criteria will be considered only in the cases where the torque allocation controller will be active.

4.4.2 Steering controller

As can be seen in figure 4.14, the steering control is comprised of two parts: the feedback part and a feed-forward part. The *feedforward part*, is the input of the driver, which is directly used as part of the steering signal. The *feedback part* is a PI controller whose input signal is derived from the addition of yaw rate error

and M_z control signal derived for the torque allocation controller. An illustration of the steering controller is presented in figure 4.15.

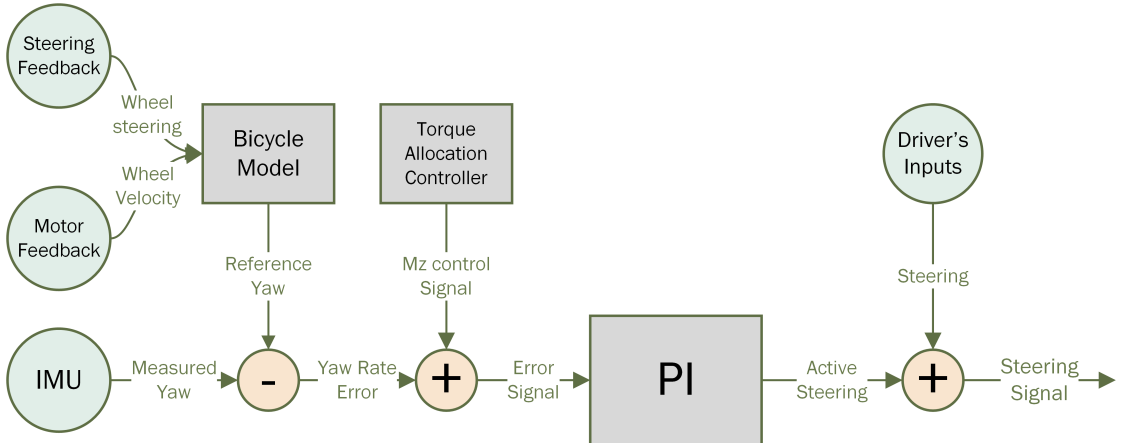


FIGURE 4.15: Steering controller block diagram

This implementation has the following advantages:

1. the feed forward part enables the driver to have direct effect on the vehicles behavior
2. the feedback control minimizes the yaw rate error which is the prime target of the steering control and
3. enables the steering controller's integral part to build up error in order to minimize yaw rate divergence and simultaneously minimize the M_z control signal.

This behavior enables the torque allocation to react fast in the first $0.5 - 1s$ after the occurrence of a fault and then gradually minimize its effect on the fault compensation by transferring all the control effort to the steering actuators. This way, the motors are not saturated and the driver has more room to maneuver.

The main asset of this approach is the combination of the torque allocation controller signal with the integral action of the steering controller which enables the aforementioned behavior. This implementation though, faces one problem; the dynamic DC offset of the yaw rate measurement that is introduced by the gyro which saturates the integral action and hence, the controller as a whole. As already

mentioned, this issue was solved by implementing a dynamic DC offset calculator which enables the controller to drive bigger distances until it saturates. This DC offset calculator though is not possible to solve the problem as a whole. For that reason, a mechanism should be developed for the reset of the integral's error periodically. Unfortunately, time limitations did not allow the implementation of such a mechanism.

Although the choice of a combination of steering and torque allocation controller seems advantageous since it enables the system to compensate faster and more efficiently, the difference between this combination approach and a simple steering controller approach is not very big, as will be seen in chapter 5. The controller combination approach was mainly introduced because the torque allocation controller was already implemented and tested. Hence, its limits and merits in combination with the steering controller needed to be tested. Unfortunately, the conditions did not allow such tests but a decent representation of its behavior can be seen in the simulated results.

4.5 Testing

Testing is the final phase of this thesis and includes the transport of the RCV in a test-track at Arlanda in order to verify and prove whether the goals of this thesis were met. In this chapter, testing safety aspects and testing limitations will be analyzed.

4.5.1 Safety measures

One major concern while testing, is safety. Since the tests themselves include fault induction while driving, the situation is prone to undesired implications. For that reason, a series of safety measures were adopted which are listed below:

- In order to minimize exposure to danger for both driver and co-driver, the models were tuned to fit the RCV's response which led to the derivation of realistic modeling results before anything was validated experimentally.

- All tests conducted in the test track, were simulated beforehand.
- Since the IMU is prompt to noise, a white noise block was added in the simulated measurements data whose magnitude was matched to the noise magnitude derived from tests conducted in the past.
- All filters and delay blocks used in the RCV were added in the Simulink model for the tuning of the controller.
- The implementation of safety switches on a joystick, which were handled by the co-driver and enabled the use of controllers only in case specific buttons were pushed, disabling otherwise any controller and enabling the driver to perform evasive maneuvers if needed.
- The people involved in the experiments know the dangers that may arise during testing and are well familiarized with the vehicle.

4.5.2 Testing limitations

Based on the RCV's structure and its wear over time, there are some limitations that cannot be violated during testing which are presented below.

- From a structural perspective, the RCV cannot exceed a velocity of 60 km/h . From a safety perspective, it is highly recommended to stay below 30 km/h while inducing faults and doing fault compensation tests.
- From the perspective of time wear, one of the RCV motors is not functional and another is working only sometimes. This results in limited velocity control and the inability to test the steering controller in combination with the torque allocation scheme.

Chapter 5

Results

5.1 Simulated results

In this chapter, the simulated results are going to be presented and commented upon. The faults that were induced in the model and produced these results were: a 40% inverted motor torque on one wheel and a wheel lock. For each fault, there is a group of four different presented cases which are presented below:

1. Initially, the response of the vehicle without any control acting upon it is presented in figure [A.1](#) and [A.5](#).
2. Next, is the response of the vehicle using the active steering controller only in figure [A.2](#) and [A.6](#).
3. Following, is the response of the vehicle using both the active steering and torque allocation controllers in figures [A.3](#) and [A.7](#), and
4. finally, the response of the vehicle using both controllers and by integrating the torque allocation controller's signal in the steering controller in figures [A.4](#) and [A.8](#).

In these simulated responses, the following format is adopted:

- The vehicle has a longitudinal velocity of 25 km/h for the duration of the tests and is limited by a simple velocity controller.

- The fault is introduced at $t = 0.5\text{s}$ and its duration is 3s .
- During the tests, the controllers that are connected to each case are active the whole time.

Inverted torque. As can be seen in figure A.2, A.3 and A.4, the yaw rate induced by the fault is compensated by the fault tolerant controller well before the driver's reaction time limit. Also, in figure A.4, the behavior that was expected to be seen is barely visible since the fault itself is not severe enough. On the contrary, the aforementioned behavior is visible in the wheel lock case.

Wheel lock. Similarly, in A.6, A.7 and A.8, the fault tolerant control compensates for the yaw rate induced from the fault, marginally before the driver's reaction time. Also, it reduces the evolution of the fault by minimizing its maximum yaw rate divergence compared to the uncompensated case (figure A.5) by less than half. Finally, by integrating the torque allocation signal to the steering controller, the controller successfully enables the motors to compensate for the fault and enforces the steering controller to take over as soon as possible in order to allow the driver to control the longitudinal velocity more efficiently. The same behavior is more intense when seen for higher velocities.

In figure 5.1, a more clear view of the vehicle's response while different control strategies are active, is presented.

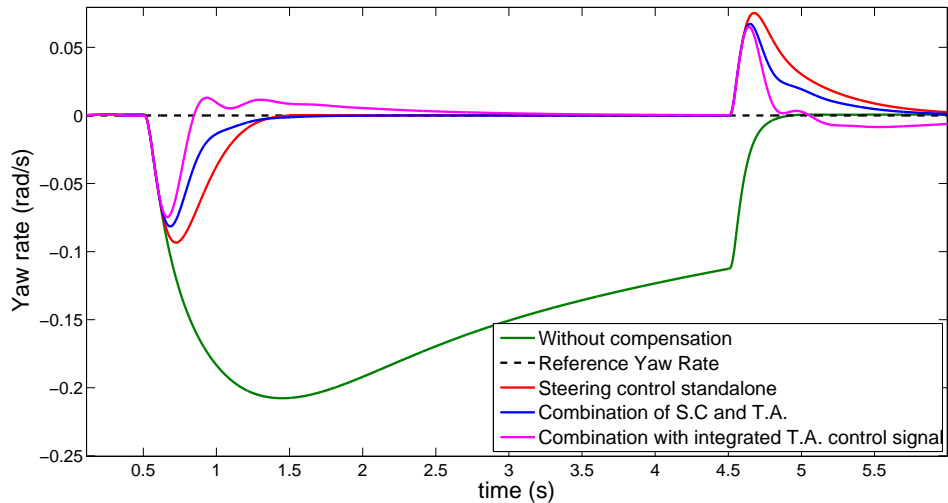


FIGURE 5.1: Yaw rate response of the vehicle for the different control strategies.

Disabling one steering actuator, was not simulated since there was not enough knowledge about the response of the wheel and how to simulate this fault. More specifically, the faulty wheel steering is affected by the vehicle's motion but there was not enough time to analyze that behavior. Thus, this test was conducted with lower velocity since the exact response of the wheel was unknown.

5.2 Measured results

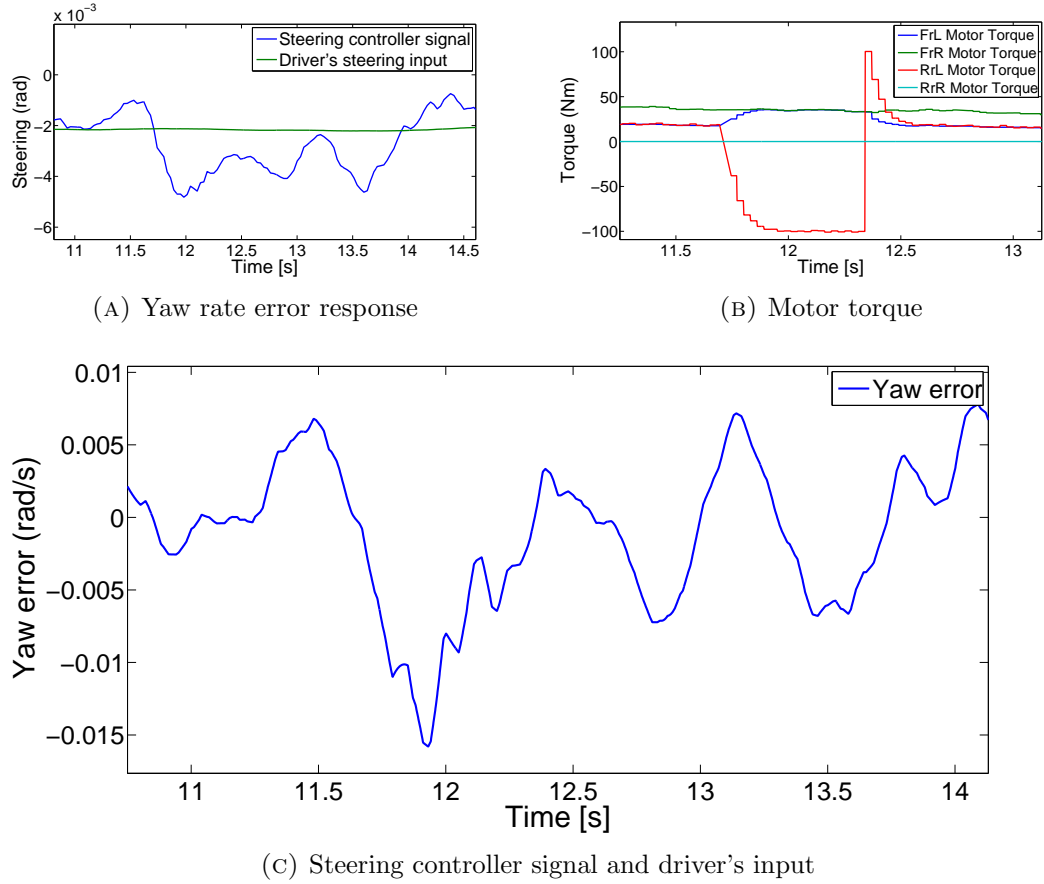
In this chapter, the measurements that are presented, were acquired in Arlanda test track. The faults that have been tested are the following:

- induction of 100 Nm on the rear left motor
- deactivation of the front right steering actuator
- locking of the rear left wheel

It should be noted at this point, that since tests were conducted by many people, time was very limited and the visits in Arlanda test track are expensive and hence rare, the tests carried out were limited to the most necessary tests. Also, the tests requiring torque allocation were not conducted because both rear motor did not function properly and the application of torque allocation with only two active motors would not give appropriate results. Finally, in this chapter, only a part of the acquired data is presented and in a shrunk version in order to make the document easier to study. The same figures exist also in appendix [B](#) with bigger dimensions.

5.2.1 Braking torque induction

In figures [5.2a](#), [5.2b](#) and [5.2c](#), the measurements of yaw rate error, motor torques and steering signal are presented. Additionally, the braking torque is induced at $t = 11.7 \text{ s}$ at longitudinal velocity of $v_x = 15 \text{ km/h}$.

FIGURE 5.2: Induction of a 100 Nm breaking torque on the rear left wheel

Since there was only very limited time to conduct all the tests and since it was deemed dangerous to conduct faults in high velocity before the same faults are studied in lower velocities, the response of the fault tolerant system was not tested in higher velocities for this fault group.

Also, the divergence in yaw rate is so small that it is hard to understand if the fault need compensation at all. More specifically, although the fault is not induced after $t = 12.4$, the yaw rate measurement shows a constant divergence from the reference. A possible explanation to this behavior is noise in the measurement induced by the road profile. Despite that, the controller reacts to any yaw rate divergence which leads to this presented behavior.

5.2.2 Wheel lock

The wheel lock is one of the most severe faults that can happen in a vehicle. As can be seen in figures 5.3b, 5.3a and 5.3c the error was induced at $t = 9.5\text{ s}$ while the vehicle had a longitudinal velocity of $v_x = 30\text{ km/h}$. Since the controller is suppressing the full evolution of the fault, it is not possible to show the fault's consequences without the fault. Also, for safety reasons it was not possible to remove the driver's input. Instead, the driver tried to keep the steering wheel as still as possible.

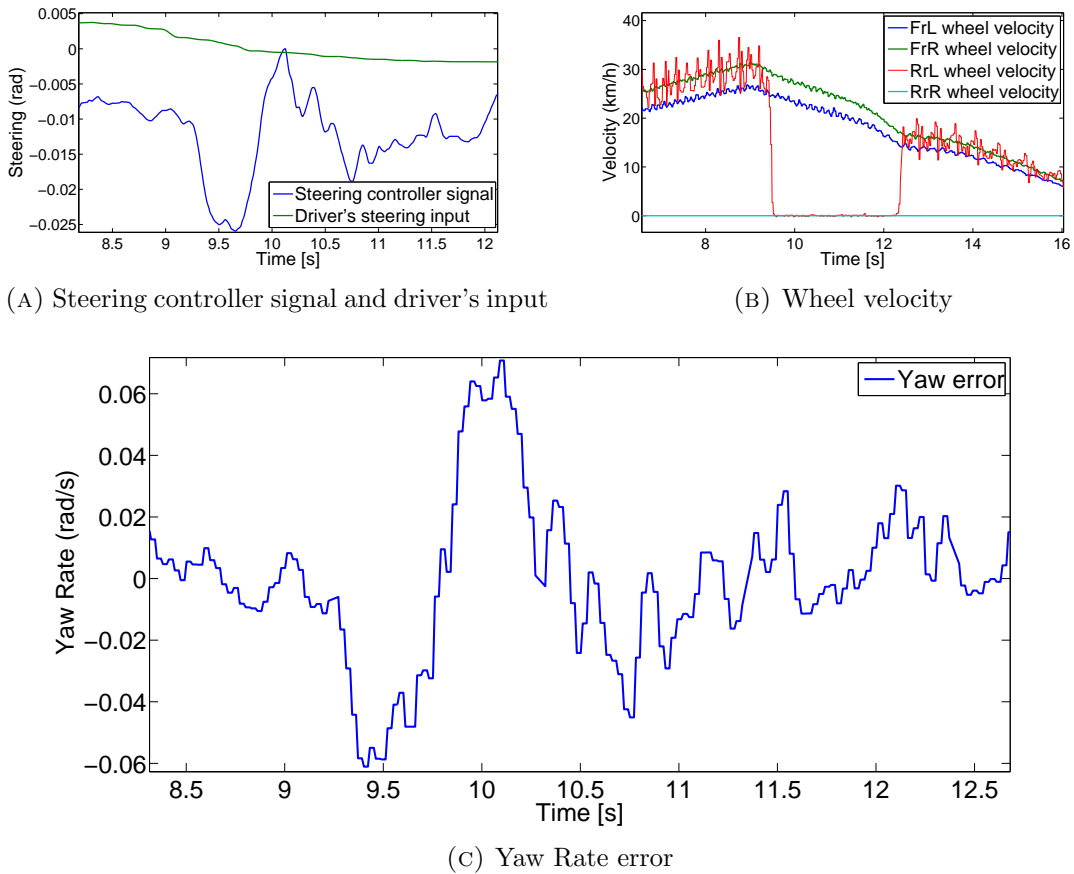


FIGURE 5.3: Locking the rear left wheel

It is important to be noted here, that the controller suppresses the fault even better than it was expected from the simulations which is a result of the difference between static and dynamic friction on the tire that was not modeled in the simulations and decreases the friction force of the tire while sliding, reducing this way the induced yaw rate.

5.2.3 Disabling one steering actuator

The final test that was conducted, included the deactivation of the front right steering actuator and the slalom drive between cones. The cones were placed on a straight line, 10 m from each other and the test was implemented with (figures 5.5) and without (figures 5.4) the steering controller active. The vehicle's longitudinal velocity was around $u_x = 12.5 \text{ km/h}$.

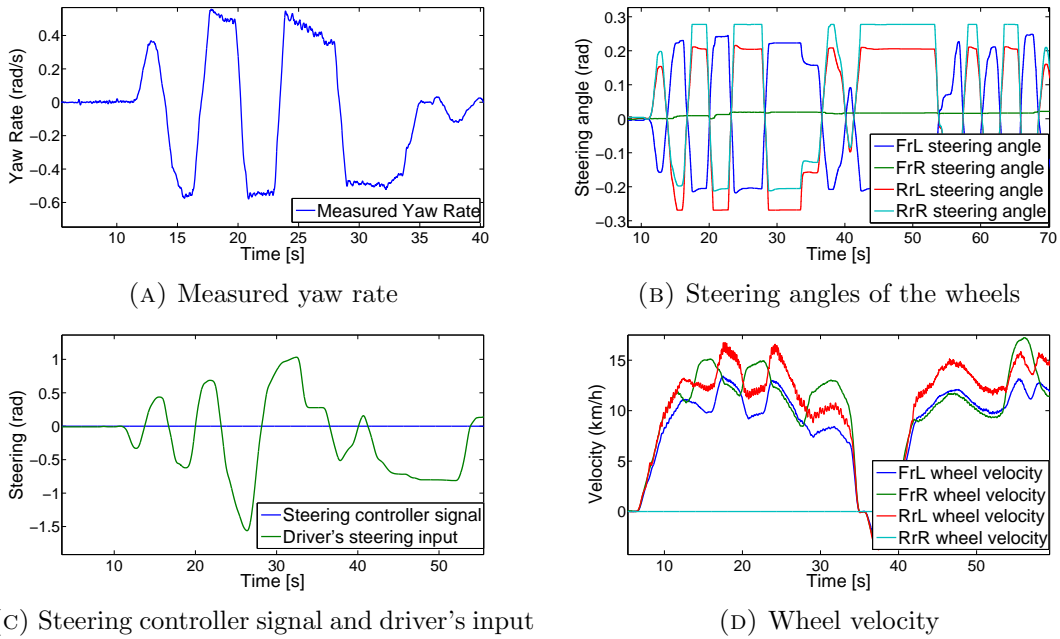


FIGURE 5.4: Deactivating the front right steering actuator

As can be seen in 5.4b, the steering angle does not increase more than a certain level since the maximum steering angle allowed in the RCV is $\delta = 26.2^\circ$. This explains the behavior of the yaw rate response in figure 5.4a which is behaving similarly. The reason why the steering actuators reach their maximum displacement is because the driver was trying to drive a slalom maneuver without success saturating the steering actuators in the process.

The same path was followed for the second test in which the steering controller was active. In this case, the controller is able to follow the reference yaw rate set by the driver as can be seen in figures 5.5b and 5.5c without the saturation of the actuators. Also, since the controller compensated for the fault, the driver continued driving normally without steering saturation problems. In figure 5.6, a closer look on the yaw rate response is presented. It can be seen that there is a

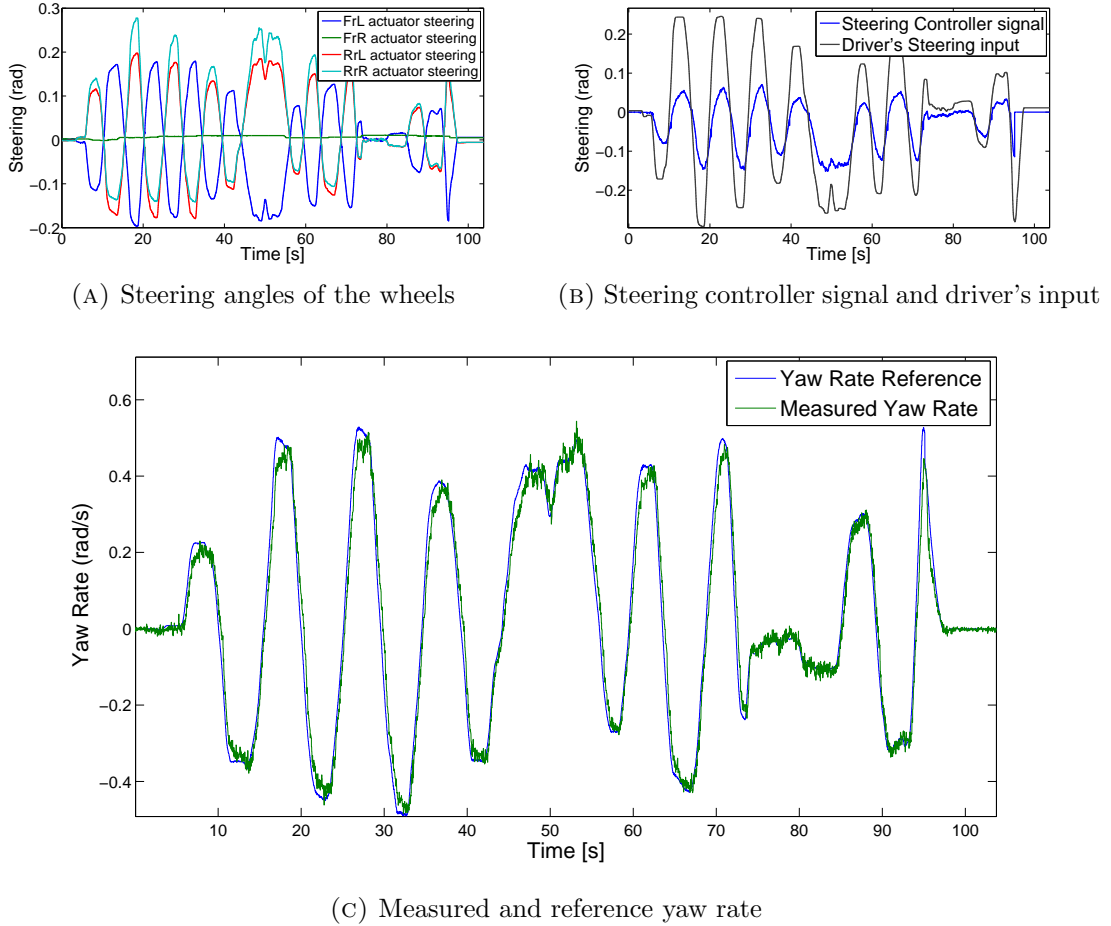


FIGURE 5.5: Deactivating the front right steering actuator

delay between reference and measured yaw rate which was expected and the delay is around $\Delta t = 200\text{ ms}$.

Finally, the aforementioned tests were conducted in very low velocities in order to avoid exposure to danger for both the vehicle and the passengers. In reality,

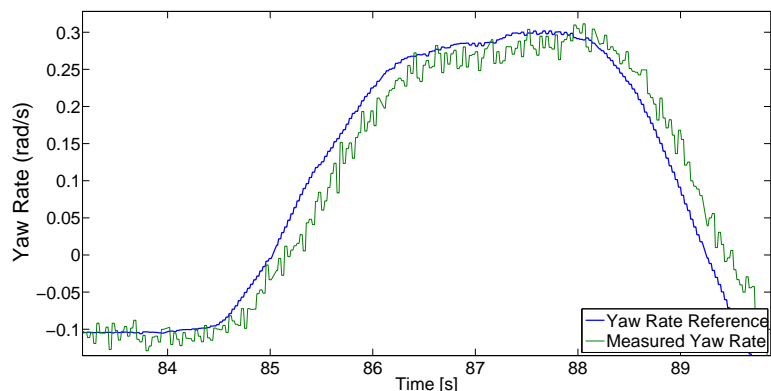


FIGURE 5.6: Measured and reference yaw rate zoomed

if a steering actuator would be deactivated in velocities higher than 40 km/h , the ramifications for a non fault-tolerant vehicle could be dire. Such tests were rejected for safety reasons.

Chapter 6

Discussion and conclusions

A discussion of the results and the conclusions that the author has drawn in the course of this thesis are presented in this chapter. The conclusions are focused on answering the research questions stated in chapter 1.6.

6.1 Discussion

As is visible in all presented experimental cases, the fault compensation controller shows encouraging results in all different experimental cases in which it was tested. More specifically, the controller fulfills the criteria based on which it was designed which were analyzed in chapter 4.4.1. More specifically:

- During the **induction of negative torque**, the yaw rate divergence was minimized, the compensation time was less than 300 ms and the driver's ability to control longitudinal velocity was maintained.
- In the case of the **wheel lock**, the two first criteria were met by minimizing the yaw rate divergence in 1 s. Unfortunately, it is not possible to control the longitudinal velocity in this faulty condition since the motors have not enough power to compensate for the friction force of the sliding tire.
- Finally, in the **disabled actuator** case, the driver was able to maintain the intended track (reference yaw rate) despite the faulty condition and without

saturating the actuators. The fault compensation time is well below the limit and the longitudinal velocity can be controlled by the driver.

To sum up, the aforementioned experiments prove that the use of a continuously active steering controller is a feasible solution which can provide efficient fault compensation.

As already discussed, the controller that was used for the tests, was designed in simulations. As can be seen in chapter 5, the simulated results show a good representation of the real vehicle's dynamics. What is worth noting here, is that the model was tuned for normal conditions and only very small parts of the tuning sample included faulty conditions. The faults that were introduced in the tuning samples were braking torques up to 100 Nm . Hence, this comparison confirms that the model can represent closely the vehicle's behavior, in more severe faulty conditions.

6.2 Conclusions

Below the research questions stated in chapter 1.6 are presented followed by their respective answers. Most of these questions have been answered in different parts of this report but for clarity reasons, are compiled here.

Question 1: *How can the chosen faults be detected? Identify the obstacles to overcome in order to achieve fault detection and what support is needed from the vehicle E/E architecture to aid fault detection?*

In the current RCV architecture, both hub-motors and steering actuators have fault detection mechanisms built-in which enable the detection of a large majority of the faults that were initially chosen. Despite that, there are some faults which in the current configuration are undetectable, namely the failure of the current sensors, the temperature sensors or the velocity sensors. The specific motor drives that were chosen for the RCV, do not have any sensor redundancy which makes it hard to detect a failure in the sensors. Hence, the requirement of sensor redundancy is set for the choice of the next motor drives.

In order to address this issue, the initial plan was to implement a fault detection mechanism outside the motor drives which would mean the addition of hardware and software, but this plan was quickly abandoned because it was deemed out of the thesis' scope and because both actuator systems are black boxes and the addition of detection mechanisms seemed inefficient and its results would not be reliable. Instead, it was chosen to clarify this finding for the choice of possible new motor drives.

A set of **obstacles** needed to be overcome in order to achieve fault detection. These obstacles are the following:

- not all faults are detectable
- addition of software and hardware for fault detection would be inefficient and unreliable
- Actuators are black boxes

The E/E **support** that is needed for the detection of these faults is the fault detection mechanisms in both steering and hub-motors.

Question 2: *How can the chosen faults be handled so as to minimize risk to driver, vehicle and surroundings? Identify the obstacles to overcome in order to achieve this and what support is needed from the E/E architecture for executing the fault handling?*

The proposed approaches for fault handling are analyzed in chapter 3.4 and are the following:

- Steering controller standalone
- Steering controller and torque allocation working in parallel
- Steering controller and torque allocation working in parallel with the additional integration of torque allocation's control signal in the steering controller, which is presented in chapter 4.4.2.

The **obstacles** that were overcome in order to develop a functional, evaluated fault tolerant controller were:

- The delay of the upright delivery.
- High noise content in the wheel velocity, lateral acceleration and yaw rate measurements.
- Dynamic DC offset in the yaw rate measurement.
- Delay in the measurements derived from the IMU.
- Limited space and time for vehicle tests.

The parts of the E/E architecture that were used were:

- The IMU-GPS
- The steering actuators
- The hub-motors which enable torque allocation for yaw rate compensation
- The use of MicroAutoBox which simplified the development process.
- CAN network

Question 3: *Is the vehicle fail operational when unintended yaw rate induction is concerned?*

After an analysis of all the important on-board systems of the RCV, possible failures that can induce unintended yaw rate on the vehicle's response were listed and tested. The tests have given the conclusion that the vehicle is fail operational for the cases it was tested. Especially for the case of the deactivated steering actuator, the controller showed very efficient compensation and allowed the driver to maneuver successfully.

Finally, it is important to be noted that the goal was to do experimental tests for the torque allocation in combination with the steering controller but time limitations did not allow. Given though that the simulations derive good results

and have proven to give trustworthy representation of reality, the combination of active steering and torque allocation controllers should respond accordingly.

Question 4: *Is the proposed active steering approach viable for a conventional vehicle?*

Supposing of course that the conventional vehicle has a steer-by-wire system installed, in order to apply this control strategy continuously, the main problem that needs to be addressed is the integration of DC offset in the steering controller. Hence, an integral minimization mechanism should be designed which will reduce the integrated DC signal over time. Given that using the compensation algorithm at this point the DC offset is $|\dot{\psi}_{offset}| < 0.0001 \text{ rad/s}$ and the integral gain is $K_I = 0.8$, the integrated offset will start affecting the behavior of the vehicle after $t > 100 \text{ s}$ by inducing a 0.008 steering signal.

Proof of the aforementioned behavior is figure 5.5c which shows that the controller does not show any signs of integrated offset signal since it is able to track the reference signal for almost 100 s without any issues.

Specifically for the case of a conventional vehicle using 2WS (which is normally the case). In order to get a better understanding of the way the wheel angles are calculated, figure 6.1 is presented. In this figure, it can be seen that the "Ackerman calculator" block uses as inputs, the position of the steering wheel, the turning point (which defines how much steering is allocated between the front and rear wheels) and the maximum angle. The output is the steering angle of the four wheels. This algorithm is designed in such a way, that enables the driver

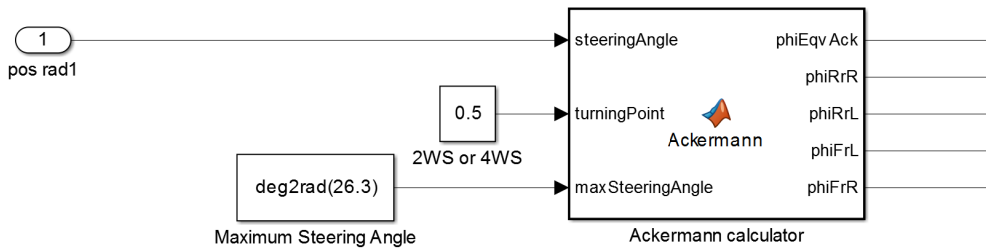


FIGURE 6.1: Ackerman angles calculation

to achieve the same steering behavior without having knowledge about the allocation of steering between front and rear wheels. In other words, the equivalent steering angle of the vehicle is constant in spite of the steering mode. Hence, this proves that the fault tolerant controller should be able to behave the same in any steering mode. The only difference between the modes is the actuation delay. If a 2WS mode is used, the steering actuators will have to travel double the distances compared to 4WS in order to achieve the same equivalent steering angle. Despite that, since the steering actuator response is described by a first order system, the actuation delay will increase only in the event that the actuators reach their maximum velocity, which (in RCV's case) is around 36 deg/s .

One special case though is rather hard for the controller to compensate. That case is the deactivation of a steering actuator. In that case, the vehicle would need to steer with only one wheel which would require high steering angle for the functioning wheel to compensate for the fault. Unfortunately, there is not enough experimental data to evaluate this case and thus will be suggested as future work.

Although the faults in conventional vehicles are not the same, the different faults examined in this thesis show that such a fault compensating approach can be of useful for many yaw rate inducing faults that might arise in a vehicle, making it this way a viable solution for conventional vehicles.

Chapter 7

Recommendations and Future work

In this chapter, recommendations on more detailed solutions and future work in this field are presented.

7.1 Recommendations

One of the initial goals was to incorporate ISO 26262. It was realized though that such implementation would not be possible in an already build prototype vehicle. Given that the goal of this research platform called RCV is to incorporate safety standards as well, the redesign of the whole vehicle is necessary to achieve that. Also, although the main focus of this thesis was to derive a fault compensating controller, it is important to be noted that an active steering approach that will enable the driver to achieve the most suiting for the circumstances driving behavior, can be achieved through an steering controller that will be continuously active and will fix the drivers input by adding the necessary signal, to achieve the intended response. That can be utilized for different driving modes or driving condition behaviors (i.e over steering on wet asphalt). Another mechanism that could help towards that direction is the torque allocation mechanism.

7.2 Future work

Since the goal of a robust, fail-operational steering system demands time and resources that this thesis did not have, here is a list of additions that can help this project further progress into that direction.

1. Changing the steering actuators to faster and more powerful ones that will improve the response time of the steering actuators minimizing this way the use of the vehicle's motors for the purposes of steering or minimizing the yaw rate divergence in faulty conditions even more.
2. Absolute homing necessary for more accurate fault compensation.
3. the IMU should be mounted on proper vibration dissipating material in order to minimize the noise which affects the controller's performance. This is especially important to the projects that use the accelerometer measurements which are prone to noise.
4. Changing the geometry of the actuator to wheel mechanical connection with an easier to steer geometry will decrease the force needed from the steering actuators to steer.
5. In order to comply with safety standards like ISO 26262, sensor redundancy is required in the motor drives since with the current configuration, possible sensor failure is impossible to detect which can result in unpredictable motor behavior.
6. More powerful motors are needed in this vehicle since they saturate easily in faulty conditions.
7. For the case of autonomous driving, a more robust controller should be tested on the RCV (i.e. Sliding mode controller).
8. The limits and merits of the steering and torque allocation controllers combination approach needs to be tested.
9. The installation of chassis mounted motors need to be examined, since the hub-motors currently installed show structural weaknesses, mainly because

of undamped vibrations which limit the vehicle's performance and range of use.

Appendix A

Appendix - Simulated results

In this chapter, all figures concerning the simulated results are presented. More specifically, figures [A.1](#), [A.2](#), [A.3](#), [A.4](#) present the simulated results derived for the induction of a braking torque on the rear left wheel and figures [A.5](#), [A.6](#), [A.7](#), [A.8](#) present the simulated results derived for the induction of a wheel lock on the rear left wheel.

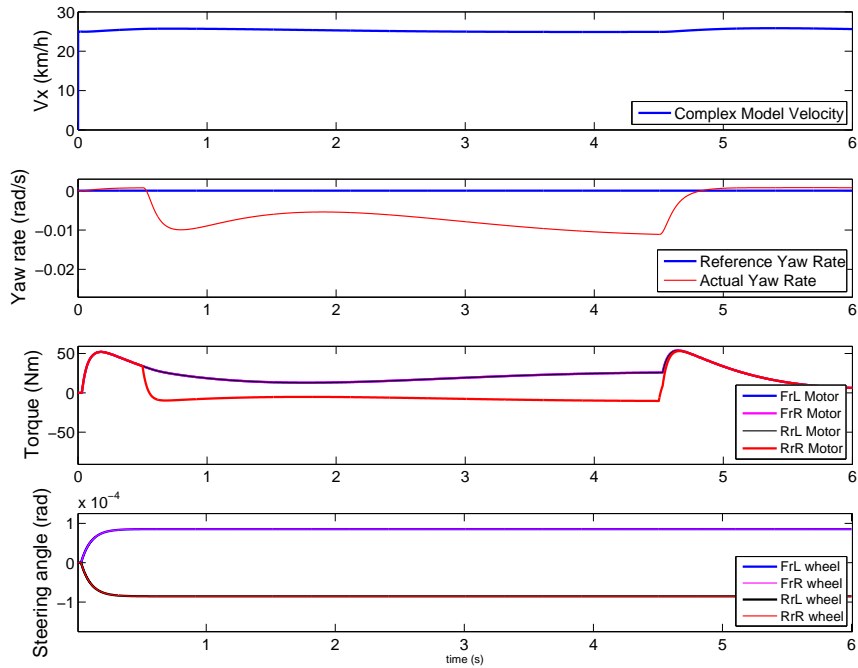


FIGURE A.1: Response of the vehicle when braking torque is induced on the rear left wheel

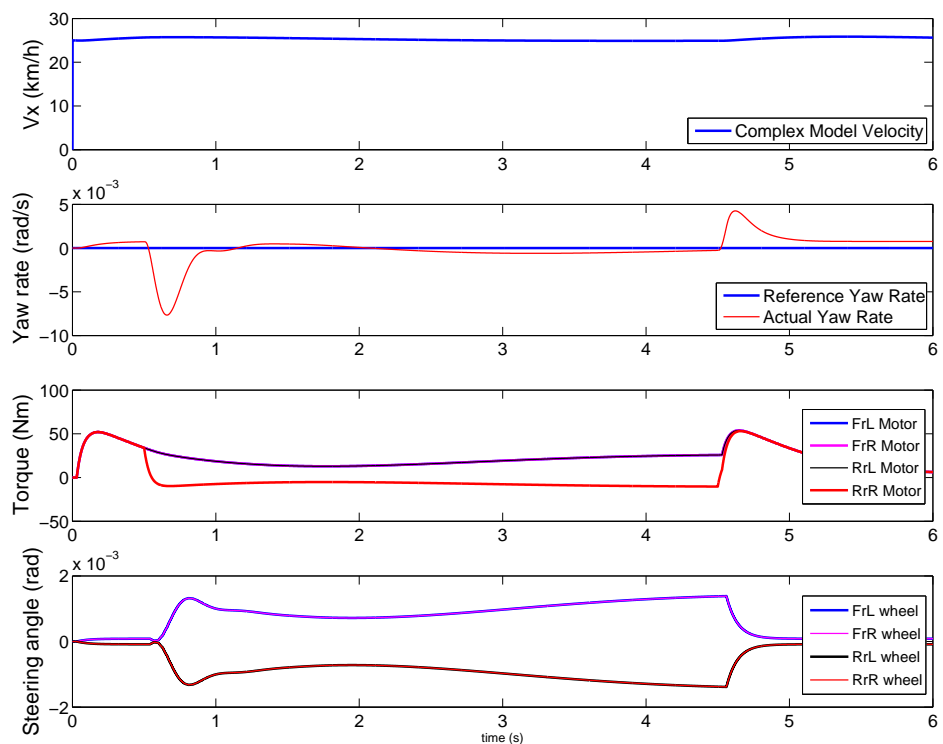


FIGURE A.2: Response of the vehicle when braking torque is induced on the rear left wheel while the steering controller is active.

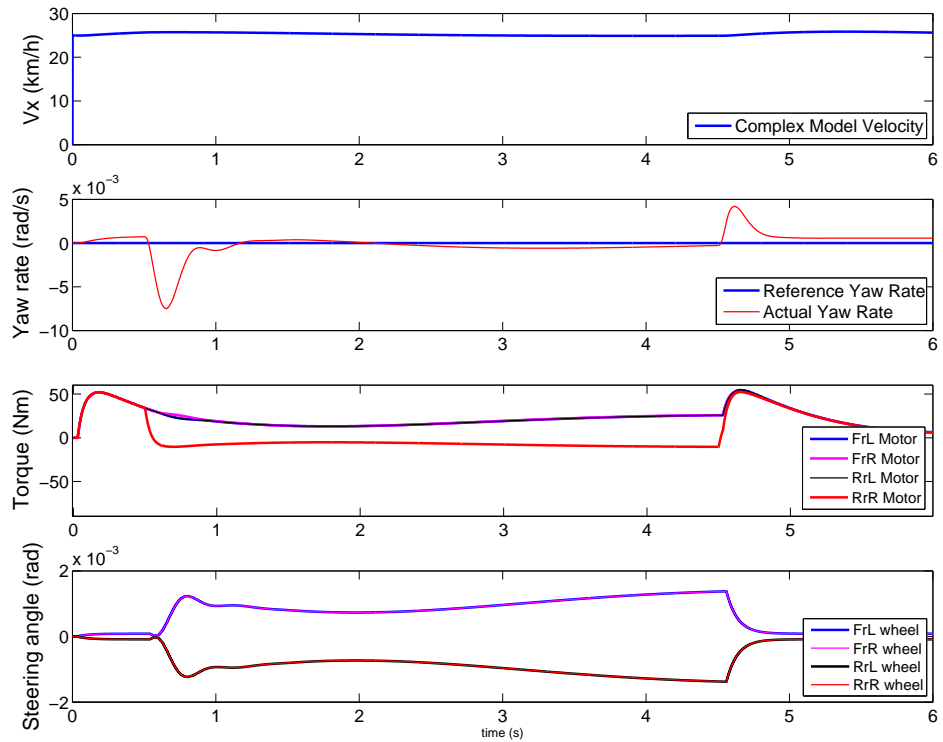


FIGURE A.3: Response of the vehicle when braking torque is induced on the rear left wheel while both steering and torque allocation controllers are active.

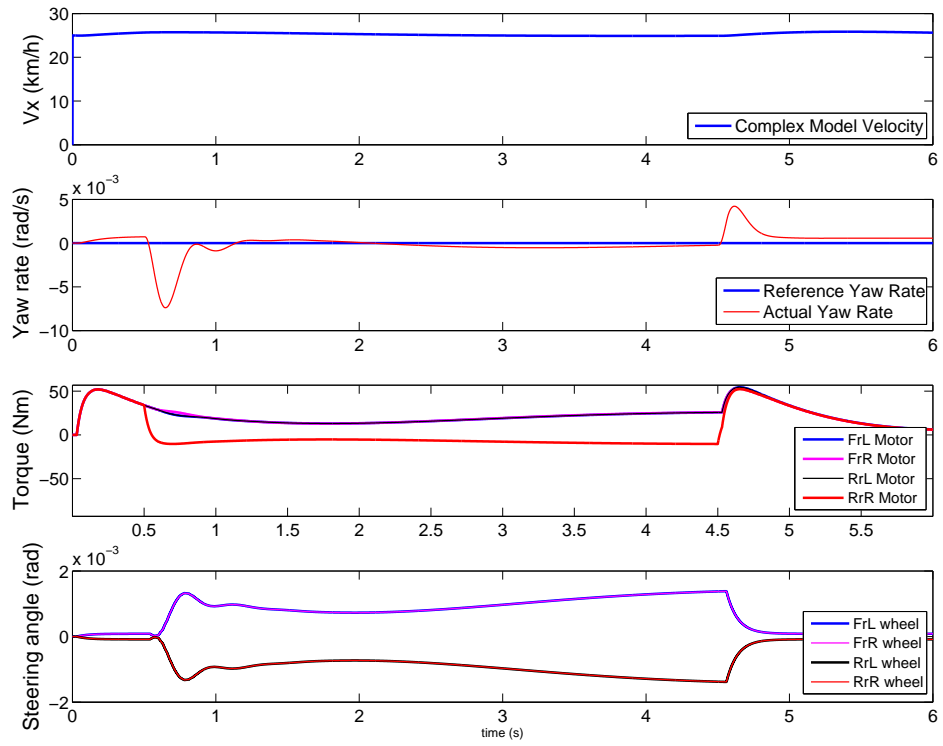


FIGURE A.4: Response of the vehicle when braking torque is induced on the rear left wheel while both controllers are active and torque allocation's control signal is integrated in the steering controller.

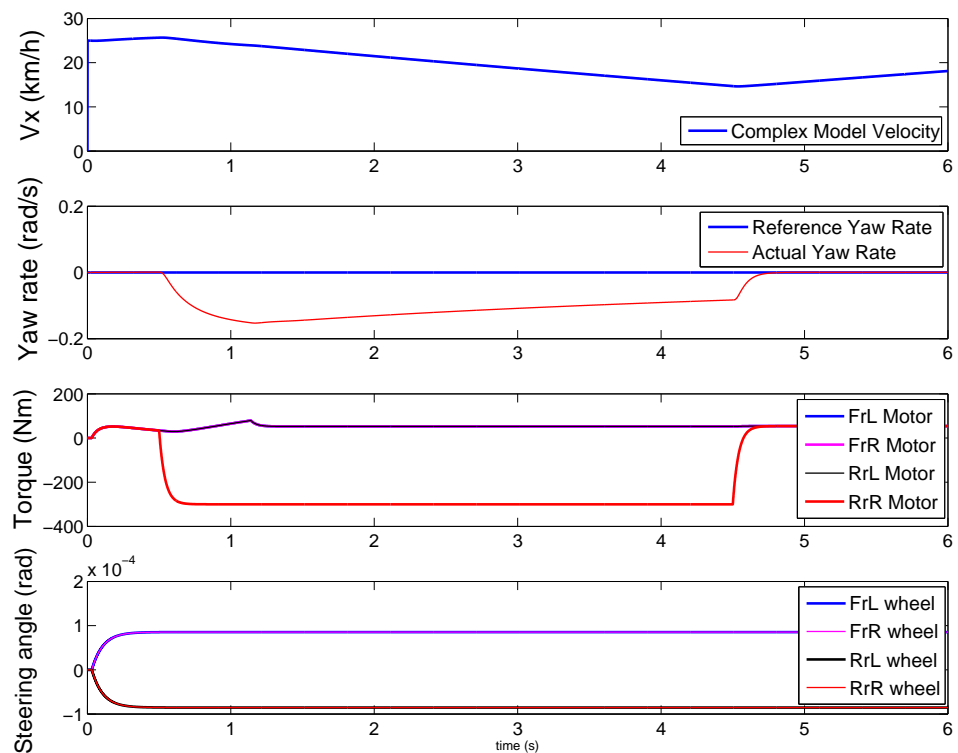


FIGURE A.5: Response of the vehicle when the rear left wheel is locked.

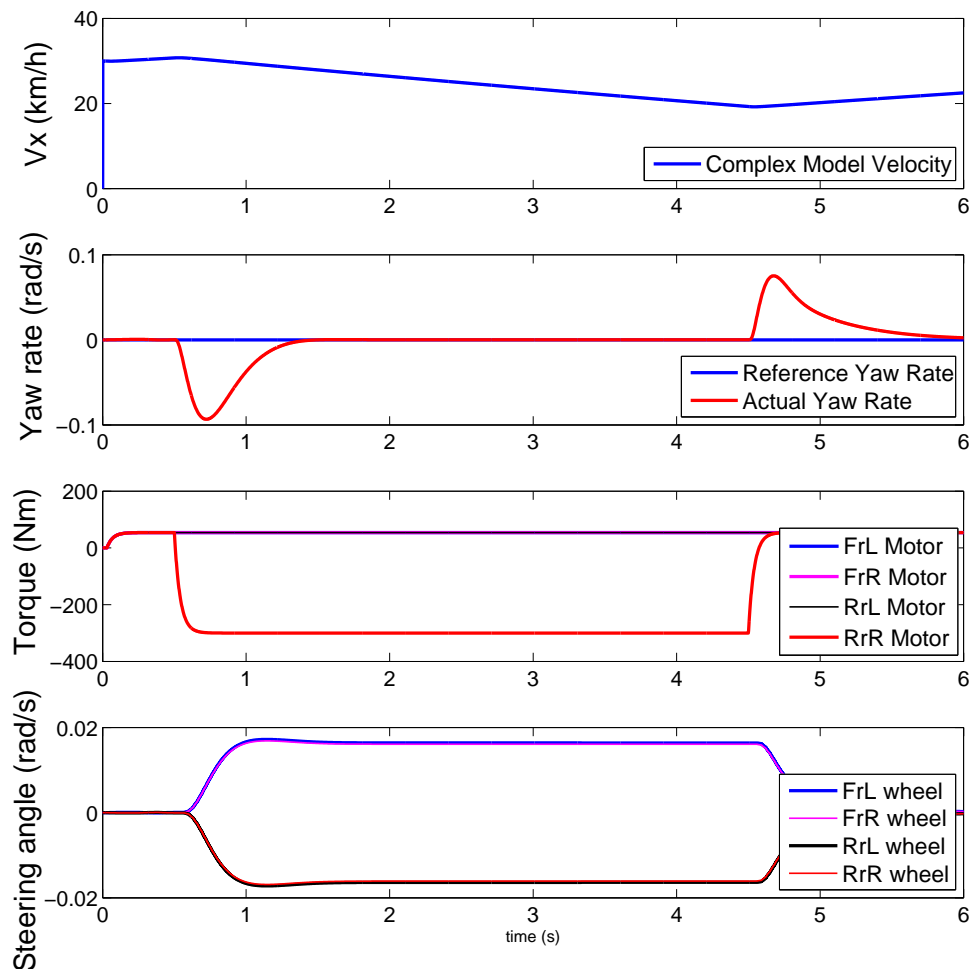


FIGURE A.6: Response of the vehicle when the rear left wheel is locked while the steering controller is active.

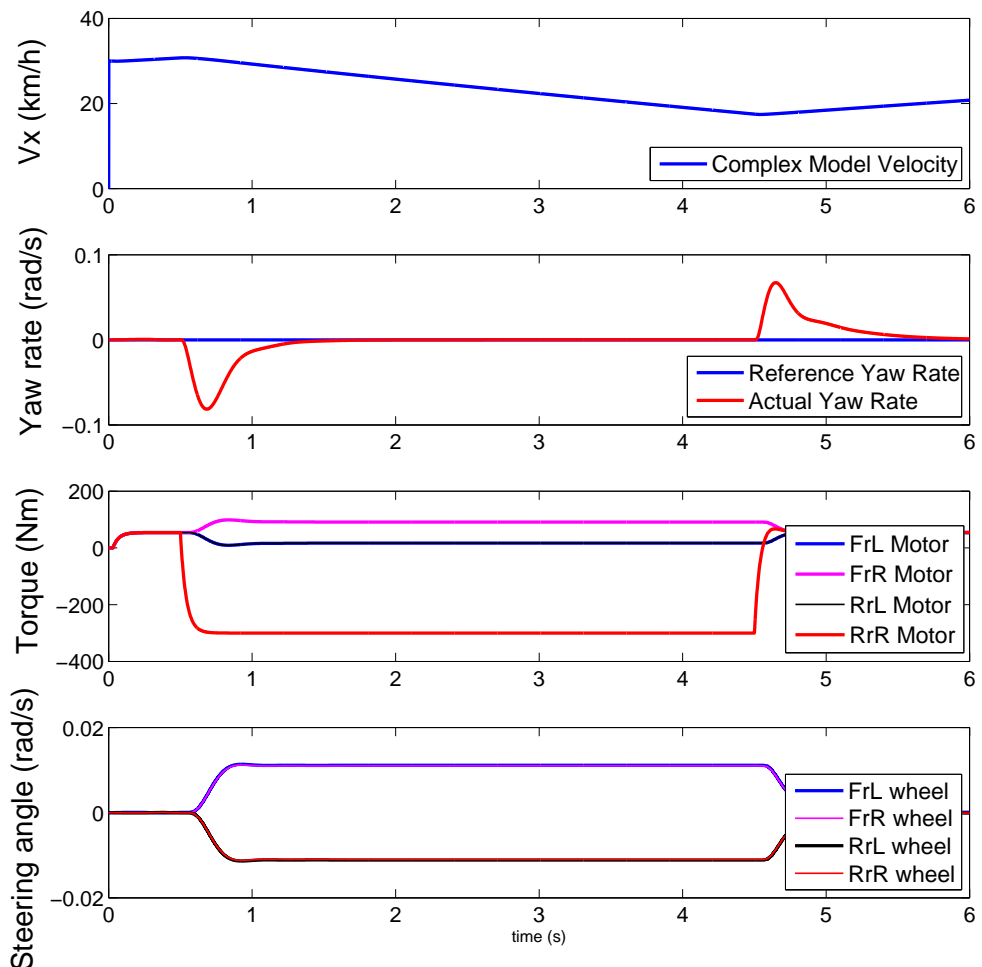


FIGURE A.7: Response of the vehicle when the rear left wheel is locked while both steering and torque allocation controllers are active.

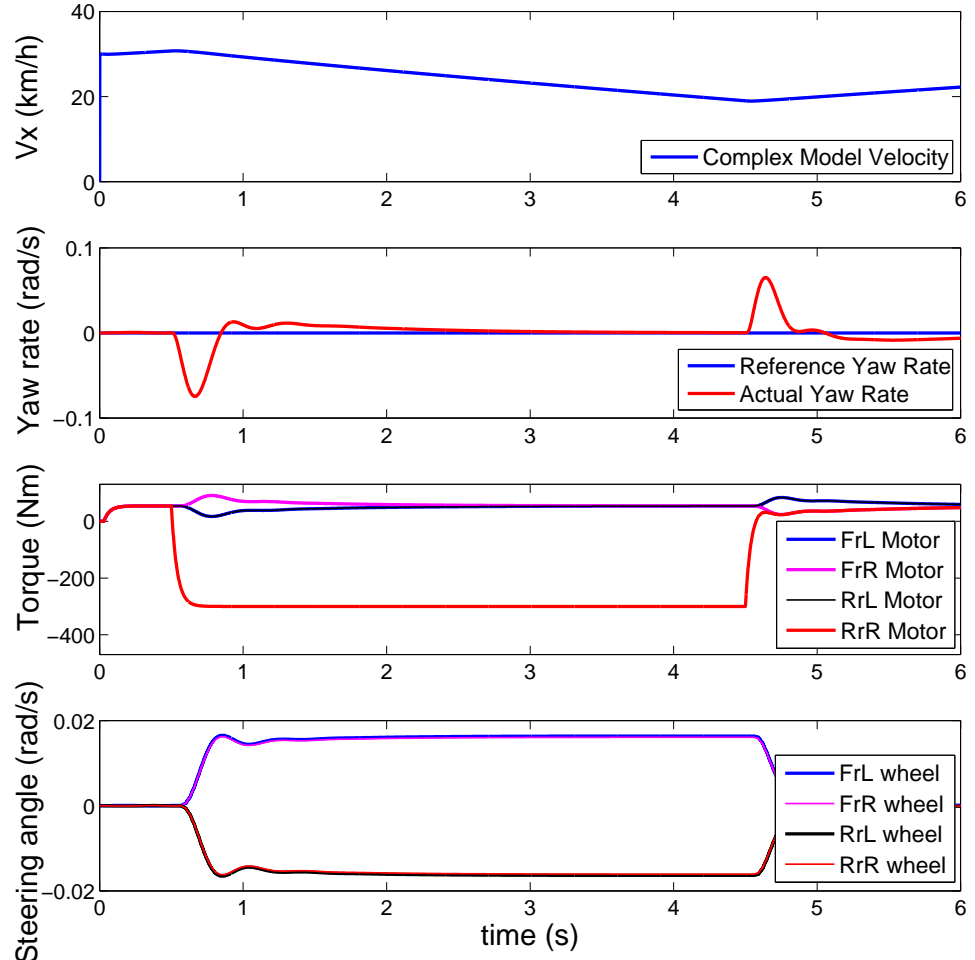


FIGURE A.8: Response of the vehicle when the rear left wheel is locked while both controllers are active and torque allocation's control signal is integrated in the steering controller.

Appendix B

Appendix B - Experimental results

In this chapter, all figures concerning experimental results are presented. More specifically, figures B.1, B.2, B.3 are the measured data acquired during conducting tests for the consequences of a 100 Nm braking torque induction on the rear left wheel. Figures B.4 ,B.5, B.6, B.7 are the measured data acquired during deactivation of the front right wheel steering actuator without the steering controller active. Figures B.8, B.10, B.9 are the measured data acquired during deactivation of the front right wheel steering actuator with the steering controller active. Finally, figures B.11, B.12, B.14 are the measured data acquired during conducting tests for the consequences of a wheel lock induced on the rear left wheel.

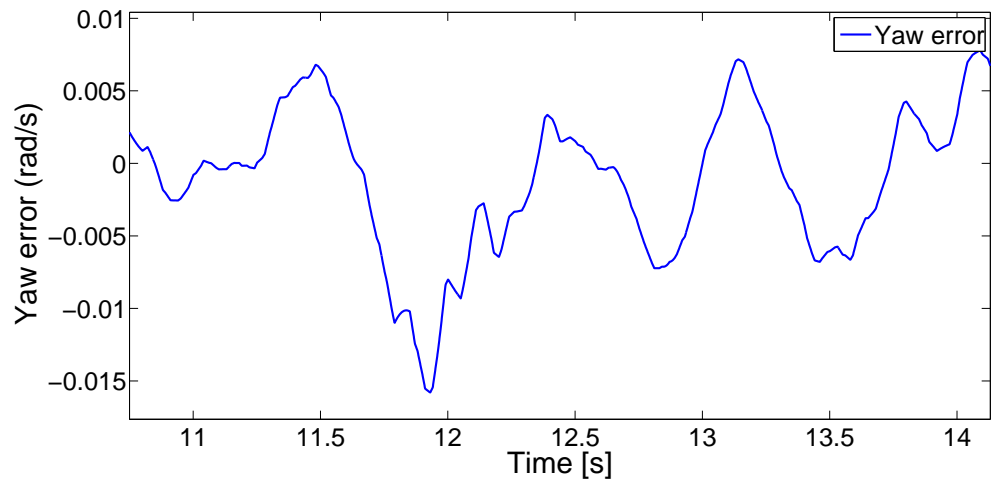


FIGURE B.1: Negative torque inductions test, yaw rate error

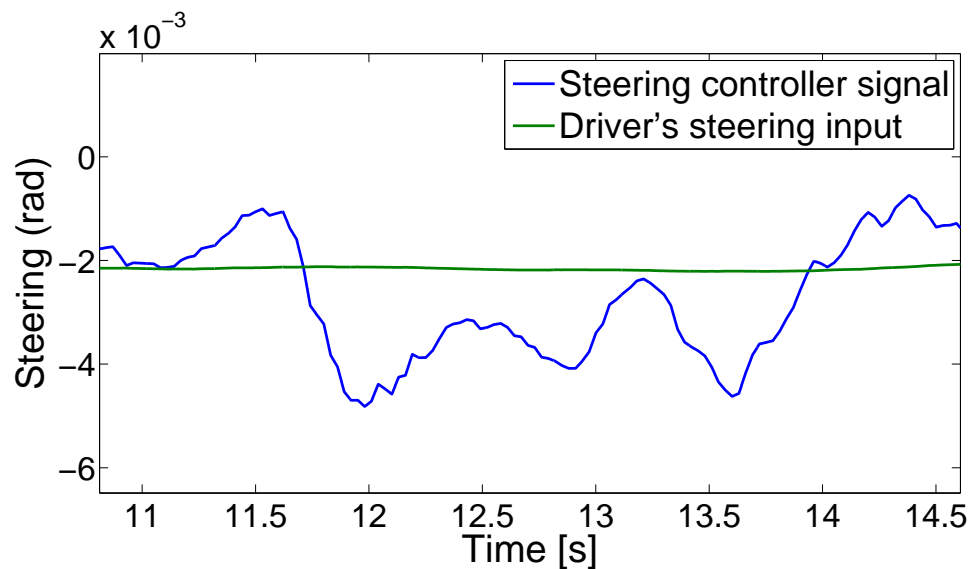


FIGURE B.2: Negative torque inductions test, steering signals

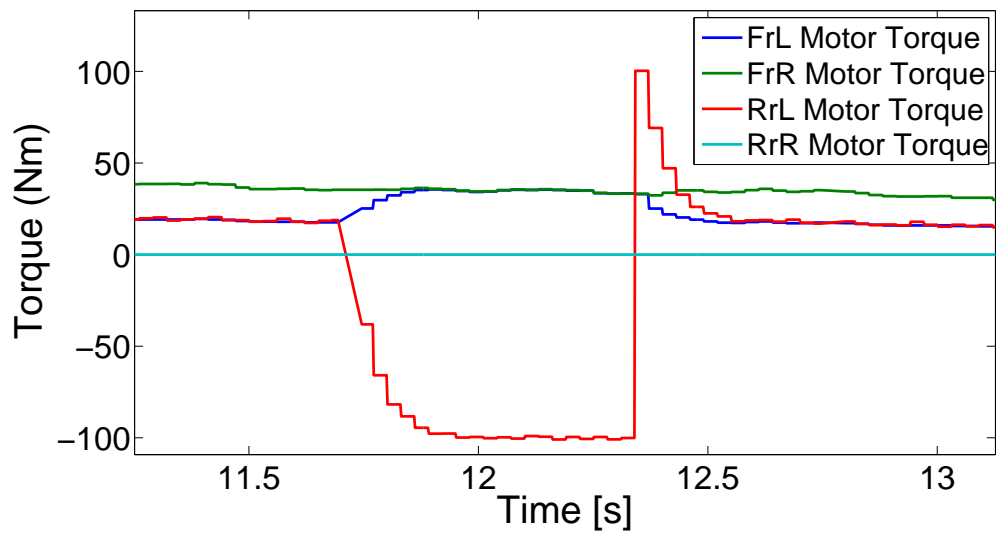


FIGURE B.3: Negative torque inductions test, motor torque

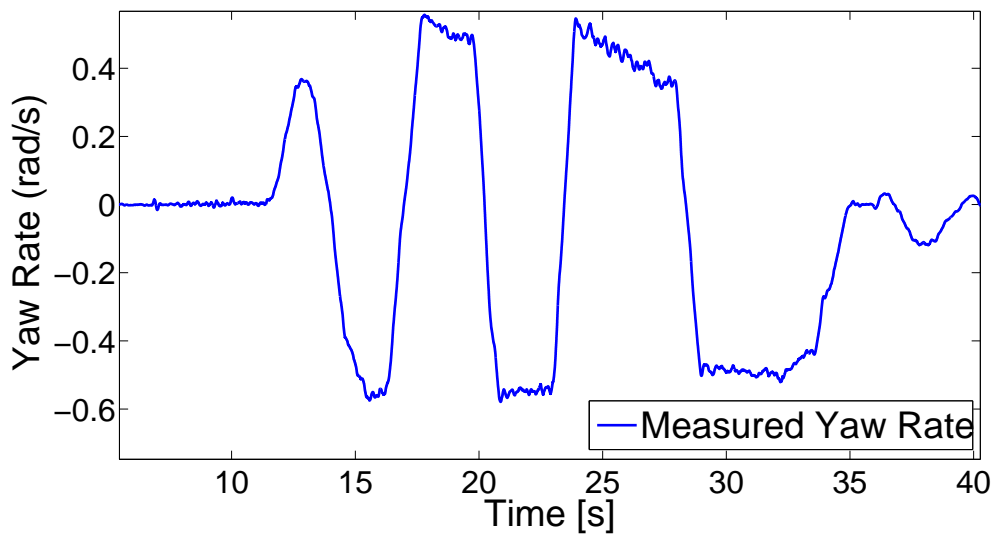


FIGURE B.4: Inverted torque fault induction response without a controller

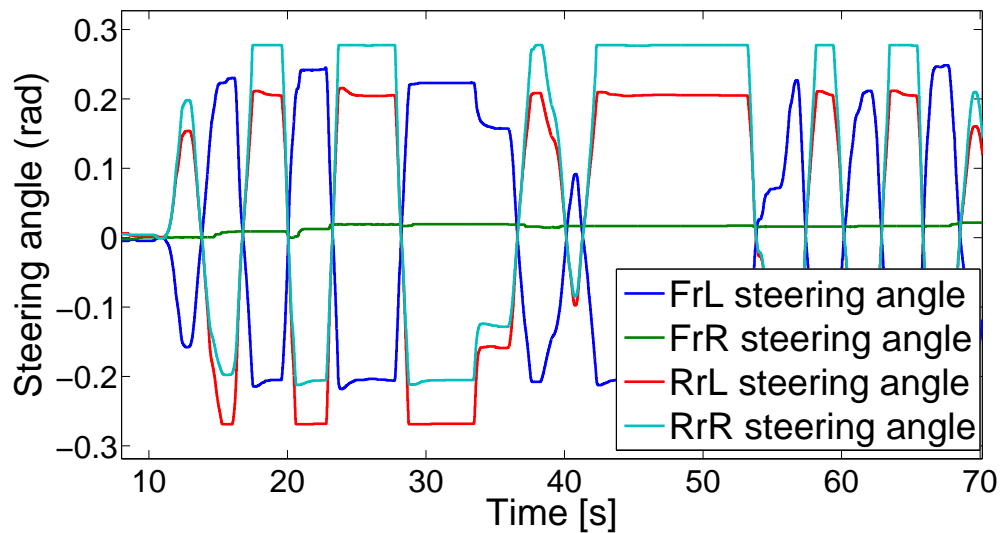


FIGURE B.5: Inverted torque fault induction response without a controller

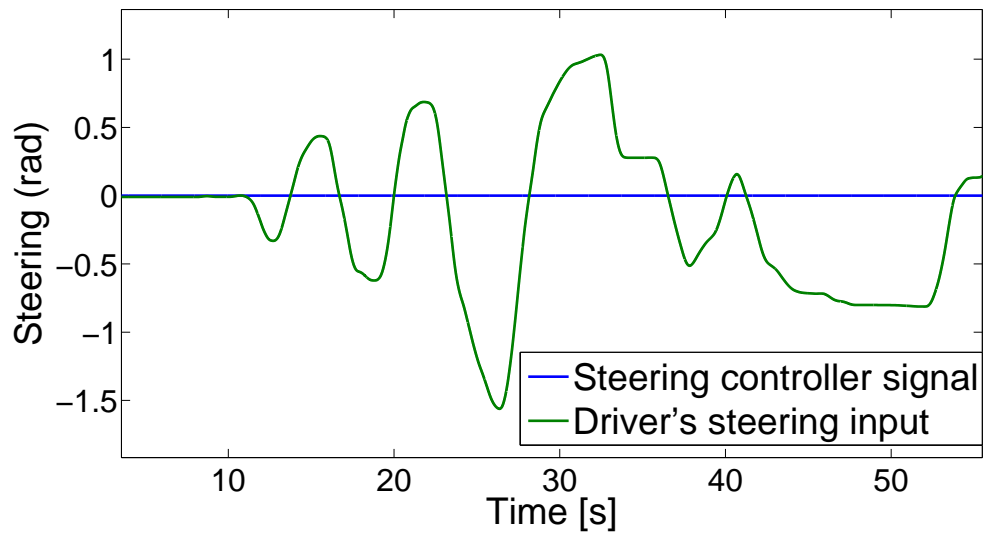


FIGURE B.6: Inverted torque fault induction response without a controller

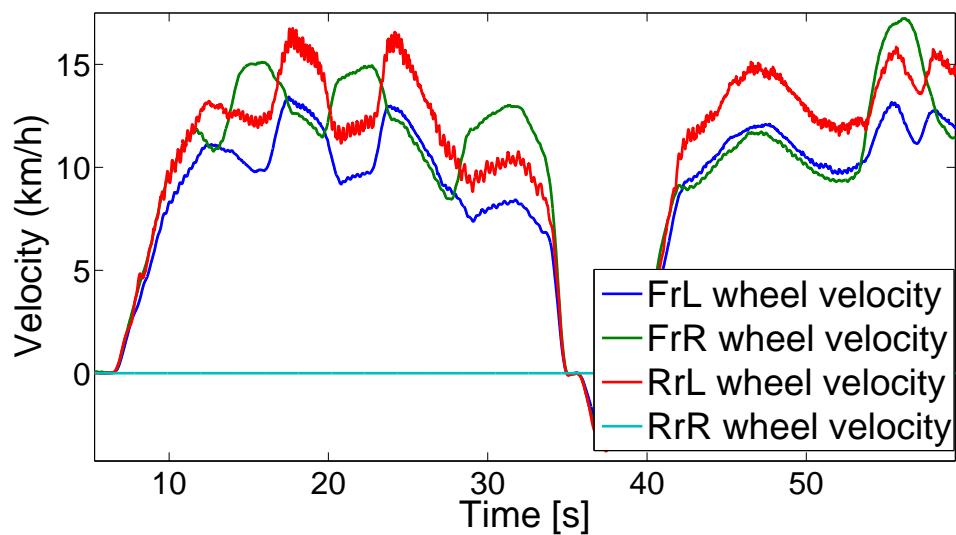


FIGURE B.7: Inverted torque fault induction response without a controller

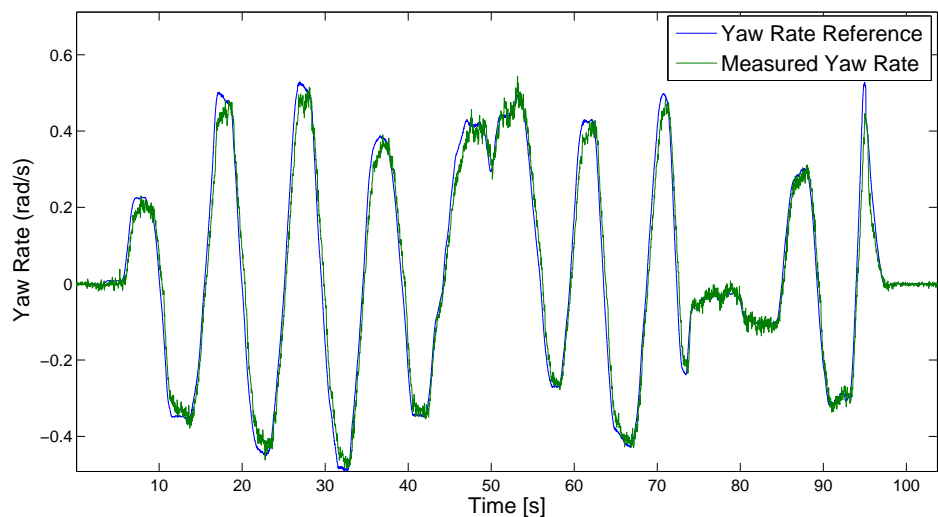


FIGURE B.8: Inverted torque fault induction response without a controller

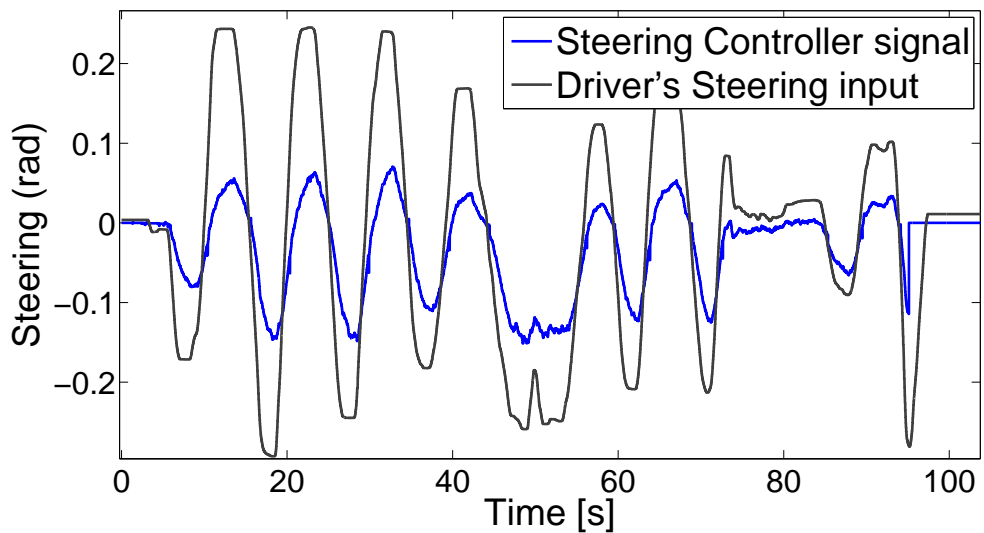


FIGURE B.9: Inverted torque fault induction response without a controller

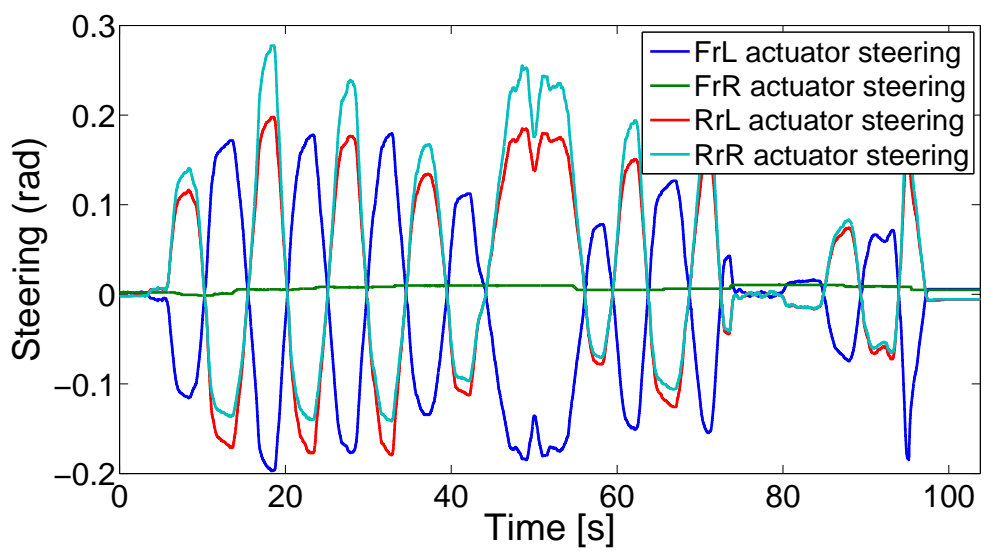


FIGURE B.10: Inverted torque fault induction response without a controller

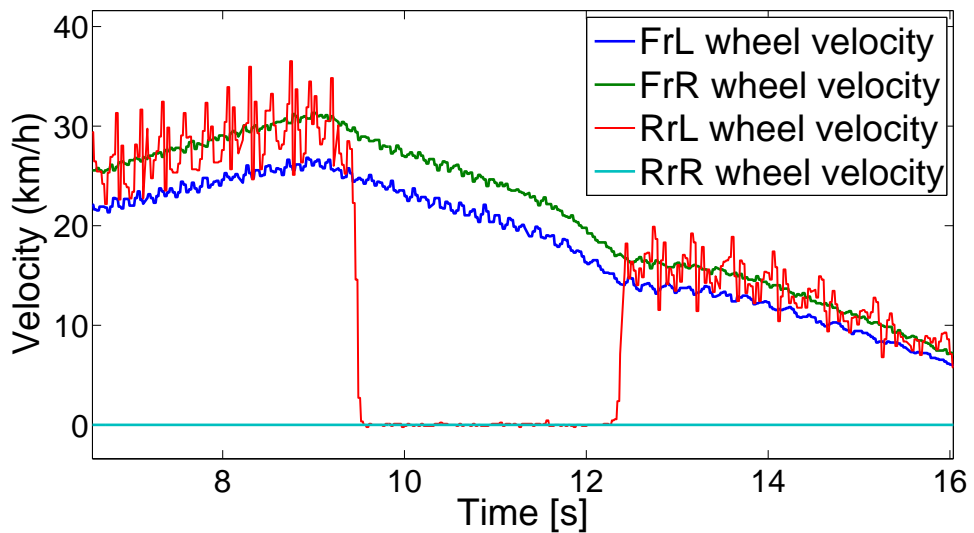


FIGURE B.11: Inverted torque fault saadinduction response without a controller

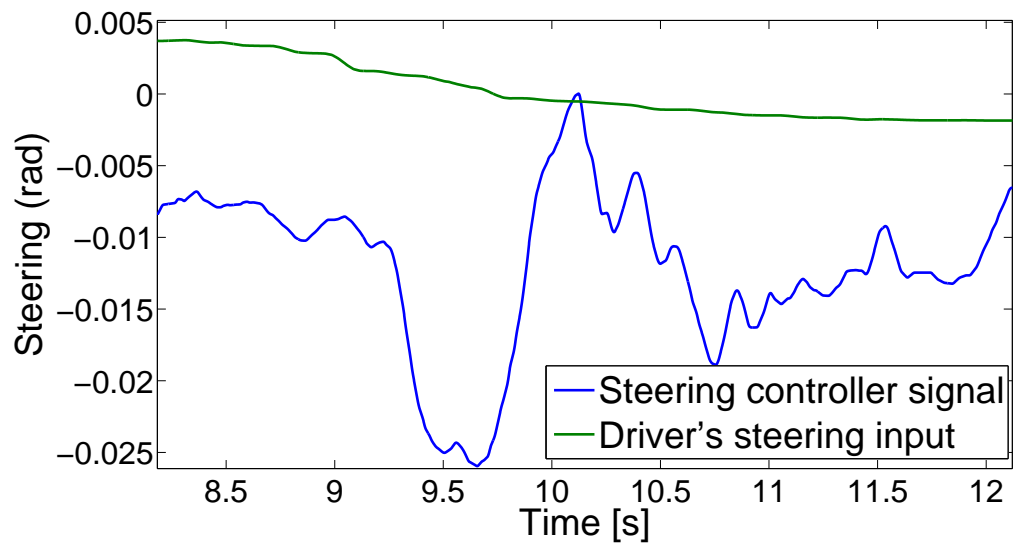


FIGURE B.12: Inverted torque fault fdainduction response without a controller

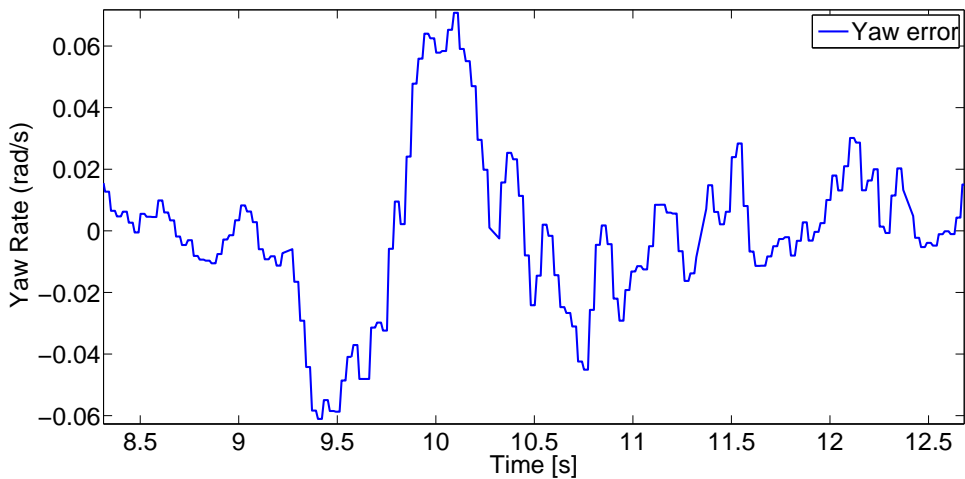


FIGURE B.13: Inverted torque fault iagnduction response without a controller

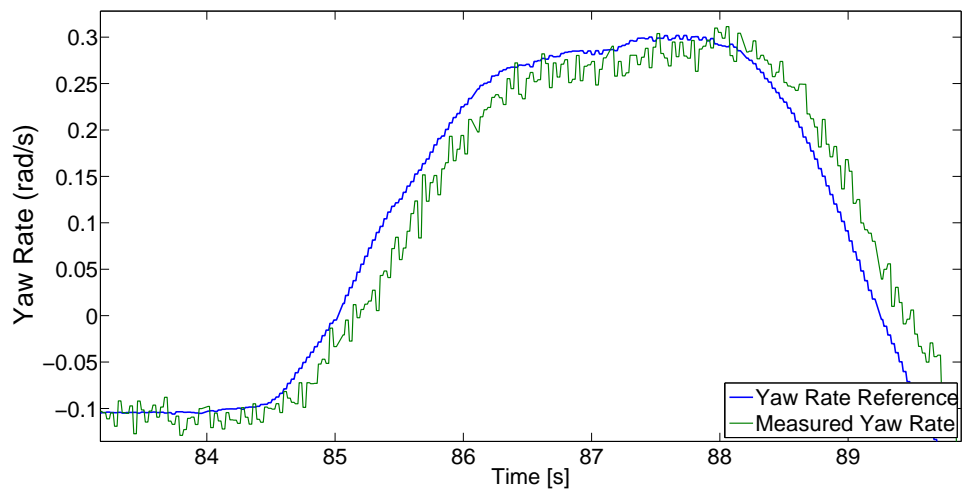


FIGURE B.14: Measured and reference yaw rate zoomed

Appendix C

Appendix C - Fault list

In this chapter, the initial list of faults is presented in tables [C.1](#) and [C.2](#).

TABLE C.1: List of fault groups 1-3.

	Failure mode	Fault	Error	Failure effect	Potential Cause(s) / Operating condition
F G 1	Open circuit (1-phase)	Connection box loose or broken strands	One phase of the WHM does not receive current	Motor torque reduced by 50 %	Poor fastening or vibration
	Open circuit (1-phase)	Blown fuse	One phase of the WHM does not receive current	Motor torque reduced by 50 %	Too high current, wrong dimension of fuse or other electrical parts malfunction
	Open circuit (2-phase)	Connection box loose or broken strands	Two phases of the WHM do not receive current	Motor torque is zero	Poor fastening or vibration
	Open circuit (2-phase)	Blown fuse	Two phases of the WHM do not receive current	Motor torque is zero	Too high current, dimension of fuse or other electrical parts malfunction
	Open circuit (3-phase)	Connection box loose or broken strands	Three phases of the WHM do not receive current	Motor torque is zero	Poor fastening or vibration
	Open circuit (3-phase)	Blown fuse	Three phases of the WHM do not receive current	Motor torque is zero	Too high current, wrong dimension of fuse or other electrical parts malfunction
F G 2	High impedance (1-phase)	Broken strands in 1 phase	reduced electromagnetic force due to smaller cumm. strand cross section	Torque reduction by 10% when 80% strands broken in 1 phase	Vibration, over temp., corrosion, poor fastening
	High impedance (2-phases)	Broken strands in 2 phases	reduced electromagnetic force due to smaller cumm. strand cross section	Torque reduction by 25% when 80% strands broken in 2 phases	Vibration, over temp., corrosion, poor fastening
	High impedance (3-phases)	Broken strands in 3 phases	reduced electromagnetic force due to smaller cumm. strand cross section	Torque reduction by 40% when 80% strands broken in 3 phases	Vibration, over temp., corrosion, poor fastening
F G 3	Short circuit - winding	Insulation has a reduced resistance	Current can flow between parallel strands of the same phase	Increase of torque by a maximum of 12 %	mechanical stress, moisture, partial discharge, overheating
	Short circuit - winding	Ground fault	Current is flowing unhindered to ground	Motor torque inverted to 25 % of healthy torque (braking torque)	Wrong or bad connection in connection box
	Short circuit - winding	Between 2 phases	Current is flowing unhindered between 2 phases	Motor torque inverted to 40 % of healthy torque (braking torque)	Wrong or bad connection in connection box
	Short circuit - mechanical deterioration	Steel fragments stick to the magnets	Current is flowing unhindered conducting fragments in air-gap	Motor torque inverted to 40 % of healthy torque	inobservant installation, worn bearing, Worn mechanical parts
	Short circuit - winding	Between 3 phases	Current is flowing unhindered between 3 phases	Motor torque inverted to 40 % of healthy torque (braking torque)	Wrong or bad connection in connection box

TABLE C.2: List of fault groups 4-7.

	Failure mode	Fault	Error	Failure effect	Potential Cause(s) / Operating condition
F G 4	Uneven magnetization	Magnets falling off	Magnetic flux of motor reduces and/or is not symmetric, local thermal	Decrease of torque by a maximum of 10 %, partial demagnetisation	mechanical stress, wrong assembly
	Too low magnetization	Demagnetized	Magnetisation gets degraded	Motor torque is reduced by up to 50 %	Wrong magnet type, overheated, overcurrent, inductive charging
	Too high magnetization	Temperature is too low for the magnets	Magnetisation gets improved	Reduction of torque towards zero torque	Extreme low temp
F G 5	Destruction of turning parts: Rotor or stator	High force acts on turning component	High force in wrong direction	Destroys the electric machine and locks the wheel	Impact
	Destruction of turning parts	Bearing deterioration/ destruction	Noise and higher friction to overcome	Less torque delivered to the wheels	Wear, overtemperature, corrosion, missalignment, bearing current, poor maintenance
	Destruction of turning parts	Shaft destruction	No torque can be transmitted to the wheels	Yaw moment is generated due to freewheeling of wheel (No torque)	Torsional resonances, overload torque, fatigue
F G 6	Control system malfunction	Incorrect temp sensor signals	Wrong temperature signals	Overheated machine cannot be detected.	Temp sensor failure
	Control system malfunction	Incorrect current sensor signals	Wrong current information in inverter leads to wrong torques/ output current	High braking torque in low speed range	Current sensor failure
	Control system malfunction	Incorrect speed sensor signals	Wrong speed information is processed in inverter to a higher/lower output voltage	Accelerating/ decelerating wheel	Speed sensor failure
F G 7	Overheated	Too high losses	electric machine can get affected	change in performance (Torque loss up to 40%)	Due to overload, other fault
	Overheated	Poor cooling	electric machine can get affected	change in performance (Torque loss up to 40%)	Initial design problem, clogged filter, broken
	Insufficient cooling	less heat transport	Coolant in system is flowing slower	higher temperatures in PMSM are reached	Corrosion, Leakage
	Insufficient cooling	less heat transport	cooling system cannot deliver required cooling power	higher temperatures in PMSM are reached	Broken radiator, contamination of water
	Insufficient cooling	Pump does not rotate	Coolant is not flowing	higher temperatures in PMSM are reached	Pump failure

Appendix D

Appendix D - Simulink model used in RCV

In this chapter, parts that were implemented for this thesis were taken from the Simulink model which is currently used in the RCV. More specifically, in figure [D.1](#), the steering controller block is presented. Inside the "Steering Control" block, is the fault tolerant controller. As can be seen, the steering signal from the output is directed to a block called "Crab2WS4WS" and is responsible for the allocation of the steering signal to the four wheels.

In figure [D.2](#), the pseudo-inverse block is presented. The fault induction is done in the "Fault induction" block. This figure represents the content of "CtrlAlloc" block in figure [D.3](#). Hence, the input signals come from the "CtrlAlloc_input2" block in figure [D.3](#).

Finally, figure [D.4](#) includes the CAN receive blocks containing the IMU measurement data which are scaled and inserted into a bus for distribution in the model. In the bottom of this figure, the yaw rate calculator is included.

Unfortunately, it is not possible to add all the parts that have been added in RCV's Simulink model for this thesis since it is hard to study in a document. Instead, the reader is encouraged to ask for the corresponding Simulink files for further analysis.

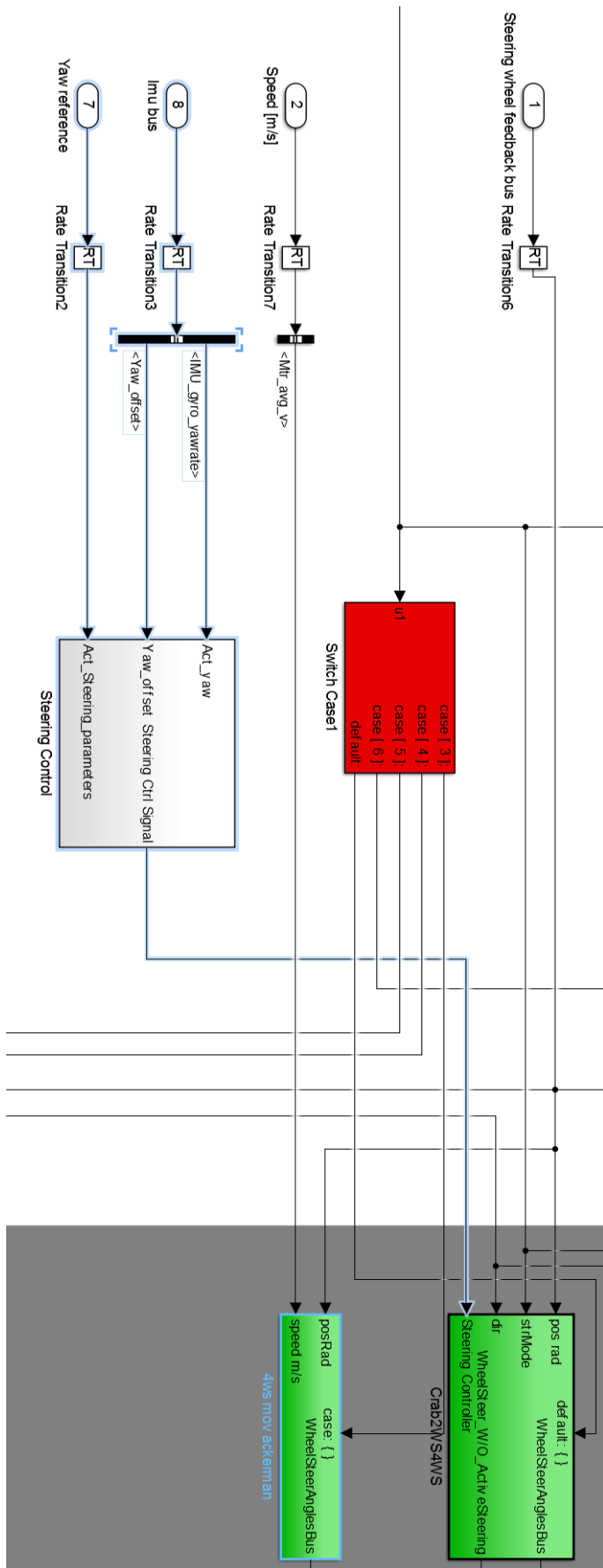


FIGURE D.1: Steering controller block.

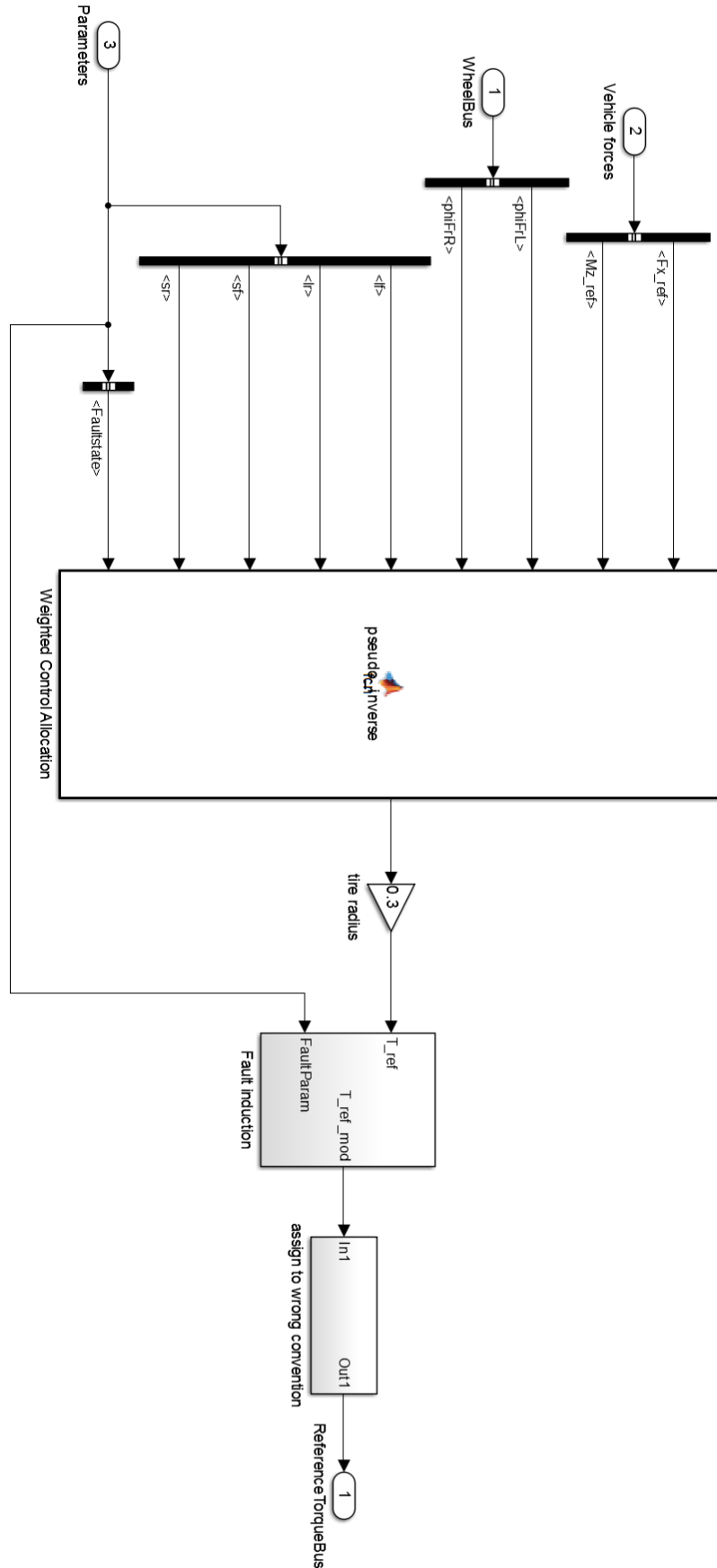


FIGURE D.2: Pseudo-inverse block.

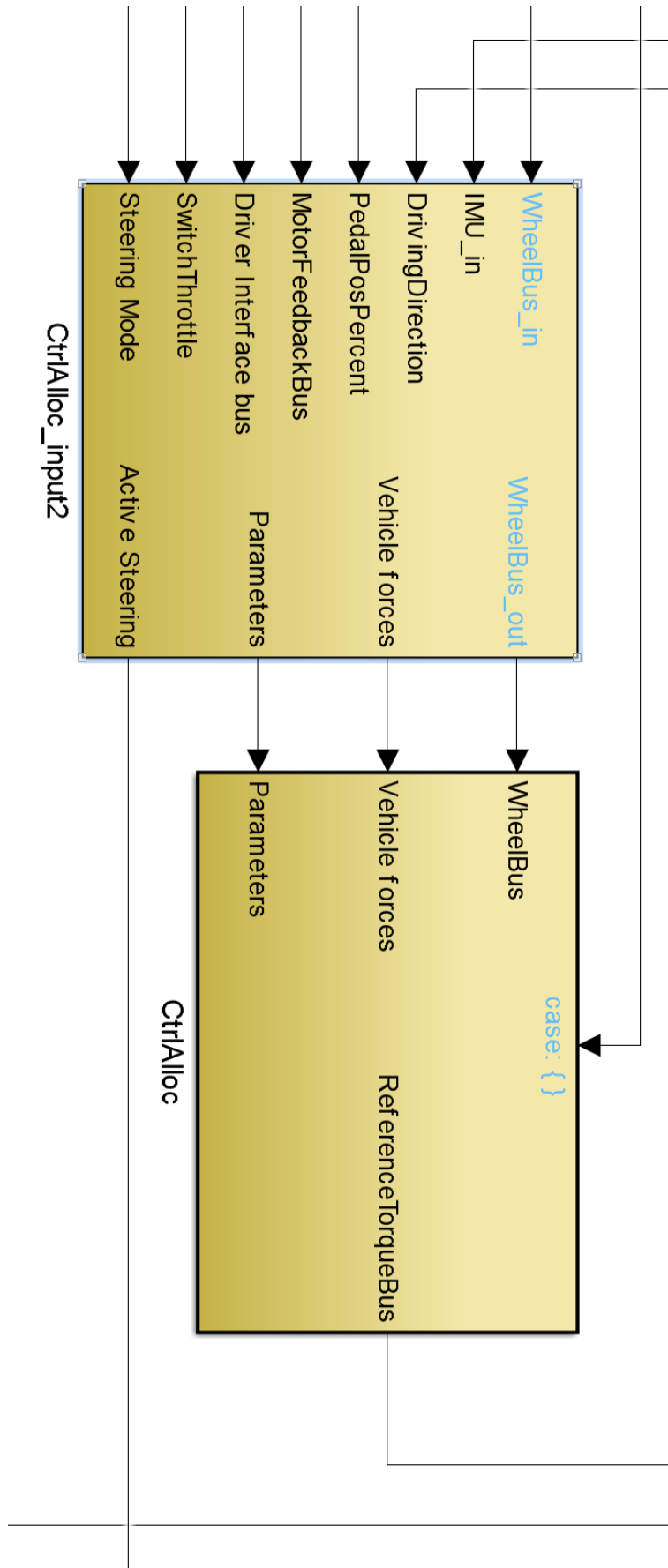


FIGURE D.3: Torque allocation blocks.

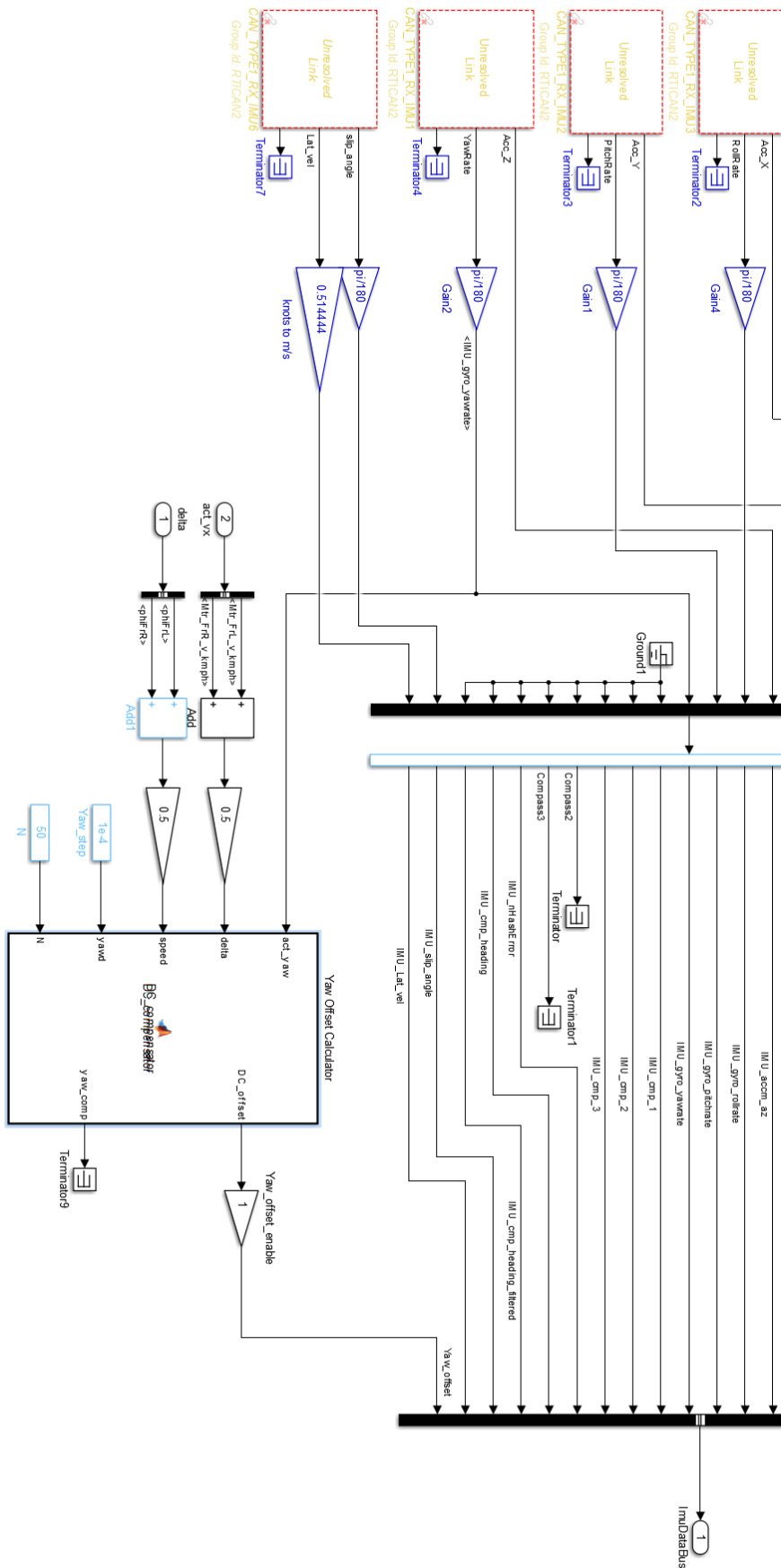


FIGURE D.4: IMU data receive block.

Bibliography

- [1] Daniel Wanner, Johannes Edrén, Mats Jonasson, Oskar Wallmark, Lars Drugge, and Annika Stensson Trigell. Fault-Tolerant Control of Electric Vehicles with In-Wheel Motors through Tyre-Force Allocation. In *11th International Symposium on Advanced Vehicle Control, 9 - 12 September 2012, Seoul, Korea*. Japan Society of Mechanical Engineers (JSOE), 2012. URL <http://kth.diva-portal.org/smash/record.jsf?pid=diva2%3A539153&dswid=564>.
- [2] Daniel Wanner, Annika Stensson Trigell, Lars Drugge, and Jenny Jerrelind. Survey on fault-tolerant vehicle design. In *26th Electric Vehicle Symposium, (EVS26), Los Angeles, CA, May 6-9, 2012*, 2012. URL <http://kth.diva-portal.org/smash/record.jsf?pid=diva2%3A539161&dswid=-6206>.
- [3] Daniel Wanner. *Faults and their influence on the dynamic behaviour of electric vehicles*. PhD thesis, 2013. URL <http://kth.diva-portal.org/smash/record.jsf?pid=diva2%3A654994&dswid=-4001>.
- [4] Daniel Wanner, Lars Drugge, and Annika Stensson Trigell. Fault classification method for the driving safety of electrified vehicles. *Vehicle System Dynamics*, 52(5):704–732, April 2014. ISSN 0042-3114. doi: 10.1080/00423114.2014.889317. URL <http://www.scopus.com/inward/record.url?eid=2-s2.0-84901643352&partnerID=tZ0tx3y1>.
- [5] Yonghui Liao. Analysis of fault conditions in permanent-magnet in-wheel motors, 2011. URL <http://www.google.si/url?sa=t&rct=j&q=&esrc=s&source=web&cd=1&ved=0CDIQFjAA&url=http://kth.diva-portal.org/smash/get/diva2:470634/FULLTEXT01&ei=>

- 81fAUJPGH4eQtQa9s4HQDw&usg=AFQjCNF6hYhHVNA3T1KJwV-beLddjoSFTA&sig2=R9IcAKne2XL6_uG833D9YA.
- [6] O. Wallmark, M. Nybacka, D. Malmquist, M. Burman, P. Wennhage, and P. Georen. Design and implementation of an experimental research and concept demonstration vehicle. In *Vehicle Power and Propulsion Conference (VPPC), 2014 IEEE*, pages 1–6, Oct 2014. doi: 10.1109/VPPC.2014.7007042.
 - [7] P I Ro and H Kim. Four wheel steering system for vehicle handling improvement: a robust model reference control using the sliding mode. *Proc. Inst. Mech. Eng. D, J. Automob. Eng. (UK)*, 210(44):335–346, June 1996. ISSN 0954-4070. doi: 10.1243/PIME\PROC\1996\210\280\02. URL <http://pid.sagepub.com/content/210/4/335.refs?patientinform-links=yes&legid=sppid;210/4/335>.
 - [8] N. Hamzah, Y.M. Sam, H. Selamat, M.K. Aripin, and M.F. Ismail. Yaw stability improvement for four-wheel active steering vehicle using sliding mode control. In *Signal Processing and its Applications (CSPA), 2012 IEEE 8th International Colloquium on*, pages 127–132, March 2012. doi: 10.1109/CSPA.2012.6194704.
 - [9] Marc Bodson. Evaluation of Optimization Methods for Control Allocation. *Journal of Guidance, Control, and Dynamics*, 25(4):703–711, July 2002. ISSN 0731-5090. doi: 10.2514/2.4937. URL <http://arc.aiaa.org/doi/abs/10.2514/2.4937>.
 - [10] J.A.M. Petersen and M. Bodson. Constrained quadratic programming techniques for control allocation. *Control Systems Technology, IEEE Transactions on*, 14(1):91–98, Jan 2006. ISSN 1063-6536. doi: 10.1109/TCST.2005.860516.
 - [11] Tor A. Johansen and Thor I. Fossen. Control allocationA survey. *Automatica*, 49(5):1087–1103, May 2013. ISSN 00051098. doi: 10.1016/j.automatica.2013.01.035. URL <http://www.sciencedirect.com/science/article/pii/S0005109813000368>.
 - [12] National Highway Traffic Safety Administration U.S. Department of Transportation. Traffic safety facts, 2014.

- [13] Petter Tomner. Design and implementation of control and actuation for an over-actuated research vehicle, 2015.
- [14] Positioning Controllers. *EPOS Positioning Controller Firmware Specification*, March 2011.
- [15] E. Baudin, J.P. Blanquart, J Guiochet, and D. Powell. Independent safety systems for autonomy. State of the art and future directions. (1):1–45, 2007. URL <http://www.google.de/url?sa=t&source=web&cd=1&ved=0CB4QFjAA&url=http://homepages.laas.fr/guiochet/telecharge/Baudin-EtatDelArt.pdf&ei=IIjKTazqGIfKswaQ6fWTAw&usg=AFQjCNHW5hnIwArE7OyfhIRo5NDNzApQIg>.
- [16] Feng Du, Ji shun Li, Lun Li, and Dong hong Si. Robust control study for four-wheel active steering vehicle. In *Electrical and Control Engineering (ICECE), 2010 International Conference on*, pages 1830–1833, June 2010. doi: 10.1109/icece.2010.450.
- [17] Yuri Shtessel, Christopher Edwards, Leonid Fridman, and Arie Levant. *Sliding Mode Control and Observation*. Springer New York, 2014. ISBN 978-0-8176-4892-3. doi: 10.1007/978-0-8176-4893-0. URL <http://link.springer.com/10.1007/978-0-8176-4893-0>.
- [18] G. Monsees. *Discrete-time Sliding Mode Control*. 2002. ISBN 9789077017838. URL <https://books.google.com/books?id=ly7xAQAAQAAJ>.
- [19] Targetlink Product Management. *Modeling Guidelines for MATLAB/Simulink/Stateflow and TargetLink*.
- [20] Youngho Park, Jihwan Kim, and Hyeong-cheol Lee. Offset Compensation Algorithms for the Yaw Rate and Lateral Acceleration Sensors. In *SAE Technical Paper*. SAE International, 2007. doi: 10.4271/2007-01-3561. URL <http://dx.doi.org/10.4271/2007-01-3561>.
- [21] Racelogic. *VBOX3i 100Hz GPS Data Logger User Guide*, May 2014.